AD-A174 532 FUNDAMENTAL STUDIES OF BETA PHASE DECOMPOSITION MODES IN TITANIUM ALLOYS (U) CARNEGIE MELLON UNIV PITTSBURGH PA DEPT OF METALLURGICAL ENGI H I AARONSON ET AL 1/1

UNCLASSIFIED 24 JAN 86 AFOSR-TR-86-2010 AFOSR-84-0303 F/G 11/6 NL

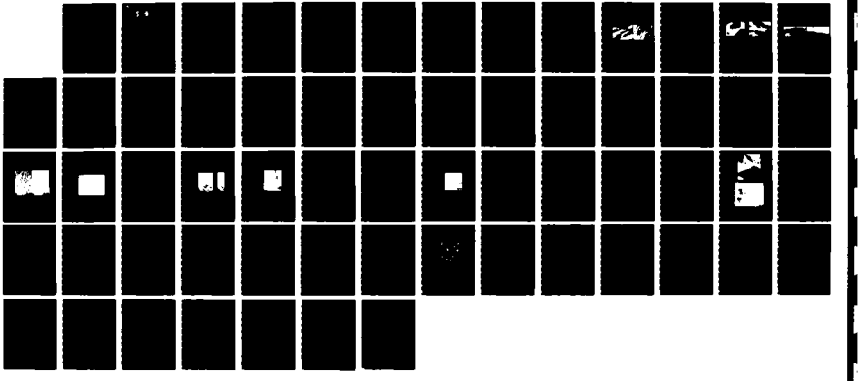

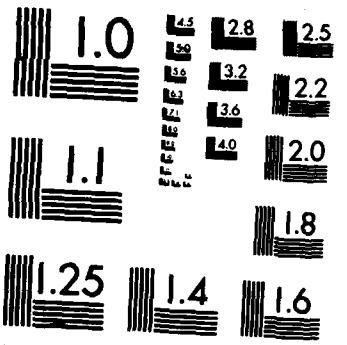

CROCOPY RESOLUTION TEST CHART
NATIONAL BUREAU OF STANDARDS-1963-A

SECURITY CLASSIFICATION OF THIS PAGE

(2)

REPORT DOCUMENTATION

DTIC ELECTE NOV 25 1986 S D

AD-A174 532

1a. REPORT SECURITY CLASSIFICATION: UNCLASSIFIED	1b.
2a. SECURITY CLASSIFICATION AUTHORITY	3. DISTRIBUTION/AVAILABILITY OF REPORT: Unlimited
2b. DECLASSIFICATION/DOWNGRADING SCHEDULE	
4. PERFORMING ORGANIZATION REPORT NUMBER(S)	5. MONITORING ORGANIZATION REPORT NUMBER(S): AFOSR-TR- 86-2010
6a. NAME OF PERFORMING ORGANIZATION: Carnegie-Mellon University	6b. OFFICE SYMBOL (If applicable):
6c. ADDRESS (City, State and ZIP Code): 5000 Forbes Ave. Pittsburgh, PA 15213	7a. NAME OF MONITORING ORGANIZATION: U.S. Air Force Office of Scientific Research
8a. NAME OF FUNDING/SPONSORING ORGANIZATION: U.S.A.F.O.S.R./NE	8b. OFFICE SYMBOL (If applicable): NE
8c. ADDRESS (City, State and ZIP Code): Bolling AFB, DC 20332-6448	7b. ADDRESS (City, State and ZIP Code): Bolling AFB, DC 20332-6448
	9. PROCUREMENT INSTRUMENT IDENTIFICATION NUMBER: AFOSR-84-0303
	10. SOURCE OF FUNDING NOS. — PROGRAM ELEMENT NO.: 61102F; PROJECT NO.: 2306; TASK NO.: A1; WORK UNIT NO.:

11. TITLE (Include Security Classification): Fundamental Studies of Beta Phase Decomposition Modes in Titanium Alloys

12. PERSONAL AUTHOR(S): H. I. Aaronson, A. M. Dalley, T. Furuhara, H. J. Lee, N. Nityanand, E. S. K. Menon

13a. TYPE OF REPORT	13b. TIME COVERED	14. DATE OF REPORT (Yr., Mo., Day)	15. PAGE COUNT
Interim Technical	FROM 10/1/84 TO 9/30/85	1/24/86	43

16. SUPPLEMENTARY NOTATION

DTIC FILE COPY

17. COSATI CODES		
FIELD	GROUP	SUB. GR.

18. SUBJECT TERMS (Continue on reverse if necessary and identify by block number): Titanium alloys, phase transformations, bainite, proeutectoid alpha, massive transformation

19. ABSTRACT (Continue on reverse if necessary and identify by block number):

A TEM study of the interphase boundary structure of proeutectoid α plates in a Ti-7.15% Cr alloy has shown that both the broad faces and edges of the plates are partially coherent. At the broad faces, misfit dislocations are 1/3<11$\bar{2}$0> whereas at the edges they are 1/3<11$\bar{2}$3>. For "normal α" plates, the dislocations are ca. 20nm apart at the broad faces and 8 nm. apart at the edges. At "black plates", the low temperature morphological variant of proeutectoid α, the dislocations are ca. 35nm. apart. Growth ledges are typically 100 - 350 nm. apart at the broad faces of "normal α" plates and ca. 700 nm. apart on "black plates". A detailed O-lattice analysis has demonstrated that a simple correlation between the misfit dislocation and the growth ledge structures does not exist. Growth kinetics studies of grain boundary allotriomorphs in Ti-3.9 w/o Co and Ti-7.15 w/o Cr have shown for the first time that the "rejector plate" mechanism is operative when the matrix phase has a bcc crystal structure. As previously predicted, however, this mechanism accelerates growth substantially less at a given homologous temperature than previous work has shown it to do in fcc matrices. The feasibility of detailed fundamental studies of the influence of β grain size upon the development of Widmanstatten α sideplates has been demonstrated. Preliminary (see reverse)

20. DISTRIBUTION/AVAILABILITY OF ABSTRACT	21. ABSTRACT SECURITY CLASSIFICATION
UNCLASSIFIED/UNLIMITED ☒ SAME AS RPT. ☐ DTIC USERS ☐	None

22a. NAME OF RESPONSIBLE INDIVIDUAL	22b. TELEPHONE NUMBER (Include Area Code)	22c. OFFICE SYMBOL
Prof. Hubert I. Aaronson Rosenstein	(412)-268-2709 767-4933	NE

DD FORM 1473, 83 APR — EDITION OF 1 JAN 73 IS OBSOLETE.

SECURITY CLASSIFICATION OF THIS PAGE

19. ABSTRACT, continued

observations have been made on sideplate evolution from grain boundary allotriomorphs by both local morphological instability and sympathetic nucleation. Plans are presented for an investigation, shortly to begin, of the crystallography and interphase boundary structure of grain boundary allotriomorphs of proeutectoid α in Ti-Cr alloys. A comparative theoretical analysis has been made of the ledgewise growth of both pearlite and bainite, using a modified version of Hillert's Fick's First Law analysis of the edgewise growth of pearlite. This analysis shows that pearlitic growth requires that the ratio of the ledge height to the inter-ledge spacing be the same on both product phases. This reproduces the growth ledges shared between ferrite and cementite recently demonstrated by Hackney and Shiflet in an Fe-C-Mn alloy. When this condition is not fulfilled, the mode of eutectoid decomposition becomes bainitic, with one product phase growing faster than the other, ultimately cutting off its access to untransformed matrix phase and requiring repeated re-nucleation of the slower growing phase at the interphase boundaries of the faster growing product phase. The fundamental external morphology of bainite is deduced to be the nodule, approximately spherical when developed in the interior of matrix grains and roughly hemispherical at grain boundaries. The plate- and allotriomorph-shaped bainite morphologies are shown to result from control of their external shape by crystals of the proeutectoid phase formed prior to initiation of the bainite reaction. The wide variety of bainite morphologies experimentally observed in different alloy systems is readily understood upon the basis of these considerations.

Interim Technical Report

from

Department of Metallurgical Engineering
and Materials Science
Carnegie-Mellon University

to

Air Force Office of Scientific Research
Electronic and Solid State Sciences
Bolling Air Force Base
Washington, DC 20332

on

Fundamental Studies of Beta Phase Decomposition Modes in Titanium Alloys

by

H. I. Aaronson, Principal Investigator
A. M. Dalley, Graduate Student
T. Furuhara, Graduate Student
H. J. Lee, Graduate Student
N. Nityanand, Graduate Student
E. S. K. Menon, formerly Graduate Student

for the period
1 October 1984 - 30 September 1985

24 January 1986

TABLE OF CONTENTS

Fundamental Studies of Beta Phase Decomposition Modes in Titanium Alloys

H. I. Aaronson, A. M. Dalley, T. Furuhara, H. J. Lee,
N. Nityanand and E. S. K. Menon*

ABSTRACT

A TEM study of the interphase boundary structure of proeutectoid α plates in a Ti-7.15% Cr alloy has shown that both the broad faces and edges of the plates are partially coherent. At the broad faces, misfit dislocations are $1/3\langle 11\bar{2}0\rangle$ whereas at the edges they are $1/3\langle 11\bar{2}3\rangle$. For "normal α" plates, the dislocations are ca. 20nm apart at the broad faces and 8 nm. apart at the edges. At "black plates", the low temperature morphological variant of proeutectoid α, the dislocations are ca. 35nm. apart. Growth ledges are typically 100 - 350 nm. apart at the broad faces of "normal α"plates and ca. 700 nm. apart on "black plates". A detailed O-lattice analysis has demonstrated that a simple correlation between the misfit dislocation and the growth ledge structures does not exist. Growth kinetics studies of grain boundary allotriomorphs in Ti-3.9 w/o Co and Ti-7.15 w/o Cr have shown for the first time that the "rejector plate" mechanism is operative when the matrix phase has a bcc crystal structure. As previously predicted, however, this mechanism accelerates growth substantially less at a given homologous temperature than previous work has shown it to do in fcc matrices. The feasibility of detailed fundamental studies of the influence of β grain size upon the development of Widmanstatten α sideplates has been demonstrated. Preliminary observations have been made on sideplate evolution from grain boundary allotriomorphs by both local morphological instability and sympathetic nucleation. Plans are presented for an investigation, shortly to begin, of the crystallography and interphase boundary structure of grain boundary al-

---

*Formerly Graduate Student, Department of Metallurgical Engineering and Materials Science, Carnegie-Mellon University and now Post Doctoral Fellow, Materials Science and Technology Division, Los Alamos National Laboratory, Los Alamos, NM 87545, USA.

lotriomorphs of proeutectoid α in Ti-Cr alloys. A comparative theoretical analysis has been made of the ledgewise growth of both pearlite and bainite, using a modified version of Hillert's Fick's Law analysis of the edgewise growth of pearlite. This analysis shows that pearlitic growth requires that the ratio of the ledge height to the inter-ledge spacing be the same on both product phases. This reproduces the growth ledges shared between ferrite and cementite recently demonstrated by Hackney and Shiflet in an Fe-C-Mn alloy. When this condition is not fulfilled, the mode of eutectoid decomposition becomes bainitic, with one product phase growing faster than the other, ultimately cutting off its access to untransformed matrix phase and requiring repeated re-nucleation of the slower growing phase at the interphase boundaries of the faster growing product phase. The fundamental external morphology of bainite is deduced to be nodule, approximately spherical when developed in the interior of matrix grains and roughly hemispherical at grain boundaries. The plate-and-allotriomorph-shaped bainite morphologies are shown to result from control of their external shape by crystals of the proeutectoid phase formed prior to initition of the bainite reaction. The wide variety of bainite morphologies experimentally observed in different alloy systems is readily understood upon the basis of these considerations.

1. INTRODUCTION

This program is primarily concerned with fundamental studies of the crystallography, morphology and kinetics of the proeutectoid α and the bainite reactions in Ti-X alloys. Interest is retained, however, in the massive mode of α formation, particularly in Ti-X systems, but also and increasingly in terms of the fundamental aspects of this transformation mode. By the term "bainite" we mean the product of eutectoid decomposition in a non-lamellar mode [1, 2]. Other definitions of bainite are currently in active use; critical consideration of these definitions forms an important part of the present program.

1985 has been a major transition year for this program at CMU. E. Sarath Kumar Menon completed all requirements for his Ph.D. thesis in May, 1985. Mr. Neeraj Nityanand has joined this program in his place and will undertake his Ph.D. thesis on the interfacial structure and crystallographic aspects of the massive transformation in a Ag-26 a/o Al alloy as soon as he has passed his Ph.D. Qualifying Examination. Mr. Hwack Joo Lee will complete his Ph.D. dissertation by the end of February, and at that time will be replaced by Mr. Tadashi Furuhara (who is already a graduate student in this Department). Mr. Furuhara will investigate the crystallography and interphase boundary structure of grain boundary α allotriomorphs and the precipitation of $TiCr_2$ at these allotriomorphs (to form bainite) in hypoeutectoid Ti-Cr alloys. Both Mr. Nityanand's and Mr. Furuhara's research programs will be "firsts" in any alloy system; they represent fundamental studies of very broad import, and the results of these studies should be generally applicable to alloys in any system undergoing a massive transformation of precipitation of grain boundary allotriomorphs, respectively.

It should also be noted in these introductory remarks that the successful completion of Dr. Menon's research on Widmanstatten sideplates and intragranular plates of proeutectoid α in hypoeutectoid Ti-X alloys largely completes this aspect of this program as envisaged at its inception. The focus of our studies on the proeutectoid αreaction in Ti-X alloys now shifts to the grain boundary allotriomorph morphology. Because orientation relationships with respect to two beta matrix grains are now involved instead of just one as in the case of intragranular or sideplates of proeutectoid α, and also because the average interphase boundary orientation of the broad faces of allotriomorphs changes frequently and varies both experimental and theoretical studies become more difficult than those widely when viewed on the scale of TEM,previously conducted on the plate morphologies of proeutectoid α. Similarly, Mr. Lee's investigation will largely conclude our research on bainite formation in association with proeutectoid α plates in Ti-X alloys. Concern with the bainite reaction in these materials will now be centered about intermetallic compound

precipitation in association with grain boundary allotriomorphs. Again, this will represent a more difficult technical problem than did its predecessor study.

2. THE PROEUTECTOID ALPHA REACTION

2.1. The Interfacial Structure of Proeutectoid Alpha Plates in Ti-X Alloys

This is the last of the five full-paper-length investigations [3, 4, 5, 6, 7] which, supplemented by two briefer studies published in Scripta Metallurgica [8, 9], constitute Dr. Menon's Ph.D. thesis. All of these publications are now either in print or in press. With the exception of this and the next item in this Report, the essentials of Dr. Menon's thesis results have been summarized in previous Interim Technical Reports.

With the exception of a brief investigation by Perovic et al [10, 11] in the Zr-Nb system, this is the first study of interphase boundary structures develpoed during a bcc -- hcp diffusional transformation in any alloy system. This study was conducted on a Ti-7.15 w/o Cr alloy. Above about 620°C, ill-formed "normal α" plates were present; sympathetic nucleation [5, 12] contributes heavily to their development. Below 620°C, well formed, low aspect-ratio "black plates" replace those of "normal α". Fig. 1a and 1b are typical TEM illustrations of the two morphologies. In another portion of this investigation, "normal α" and "black plates" were both shown to be hcp, to have the Burgers orientation relationship with respect to their parent β grains and to be of essentially the same Cr-poor composition. However, the habit plane of "normal α" plates lies near $\{111\}_\beta$ whereas that of "black plates" lies near $\{110\}_\beta$. Both the fraction of β transformable to "black plates" and the lengthening rate of "black plates" are appreciably higher than those of "normal α" when extrapolated to a common reaction temperature. The principal difference between these two variants was shown to be that "black plates" are in metastable equilibrium with β containing a much higher proportion of Cr than "normal α" plates. This results from a double inflection of the extrapolated $\beta/(\beta+\alpha)$ or transus curve consequent upon a strong tendency for clustering within the β solid solution.

Figure 1: TEM bright field micrographs illustrating the appearance of (a) *normal* α in Ti-6.6 at% Cr, β solution treated and isothermally reacted at 973 K for 1 hr and (b) *black plates* in Ti-6.6 at% Cr, β solution treated and isothermally reacted at 873 K for 2 minutes. Notice the high degree of perfection associated with the *black plates*.

Figs. 2a and b, from the present study, show misfit dislocations at α:β interfaces on "normal α" and "black plates", respectively. g.b experiments were performed to determine the Burgers vector of the misfit dislocations. This proved to be $1/3\langle 11\bar{2}0\rangle$ at the broad faces of both types of plate. The great length of "black plates" effectively prevented observations from being made on the structure of their edges. However, at the edges of "normal α" plates the misfit dislocations observed are probably of the $\langle c+a\rangle$ type, with b = $1/3\langle 11\bar{2}3\rangle$. The spacing between misfit dislocations at the broad faces and edges of "normal α" plates averaged 20 and 8 nm., respectively, whereas at the broad faces of "black plates" the spacing was about 35 nm. Only one set of misfit dislocations was seen at any of these interfaces.

Figs. 3a and b are typical examples of growth ledges on the broad faces of "normal α" and "black plates", respectively. The appreciably larger average spacing between ledges on the latter plates is clearly evident. Although considerable scatter was found in measurements of this spacing, it was estimated as 100 - 350 nm. on the broad faces of "normal α" and 700 nm. on the broad faces of "black plates", respectively.

An analysis of the misfit dislocation structure of broad faces was conducted by means of the Bollman [13] O-lattice technique. Following the approach of Hall et al [14] for fcc:bcc interfaces, all possible interfaces containing the smallest lattice vectors in the β lattice, i.e., four $a/2\langle 111\rangle$ and two $a\langle 100\rangle$, were constructed. A total of 15 interfaces was identified. The misfit dislocation structure of each was evaluated with respect to distance between parallel dislocations and the angle between the two sets of dislocations comprising each interface. Because of the aforementioned difference in composition of the β phase in equilibrium with "normal α" and "black plates", and the marked variation of β lattice parameter with Cr concentration, quite different numerical results were obtained for the two variants of

Figure 2: Ti-6.6 at% Cr, β solution treated and isothermally reacted at (a) 948 K for 1 hr and (b) 873 K for 1 hr. showing the misfit dislocations on the α:β interfaces of *normal* α plates and *black plates* respectively. Notice the change in the dislocation spacing near the edge of the plate in (b)

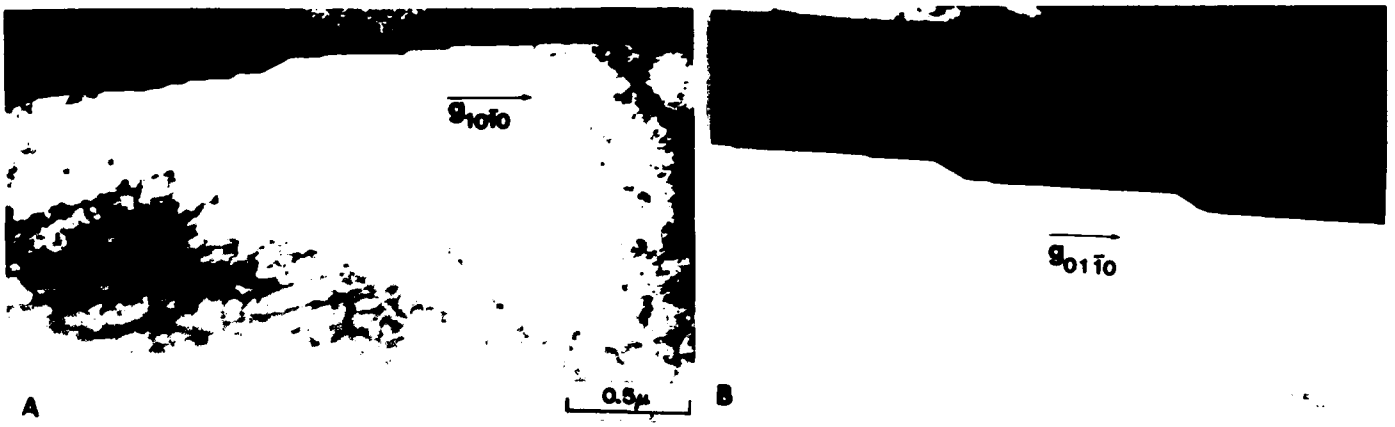

Figure 3: Ti-6.6 at% Cr, β solution treated and (a) isothermally reacted at 973 K for 2 hrs and (b) isothermally reacted at 858 K for 30 minutes, showing the growth ledges on the α:β interfaces of *normal* α plates and *black plates* respectively.

proeutectoid α morphology. Table I shows the results obtained for "normal α" and Table II presents the equivalent results for "black plates". It is seen that a number of interfaces for each type of proeutectoid α are different variants of the same crystallographic form. Thus only four forms of interphase boundary were obtained for "normal α" and five for "black plates".

Connecting the results of the O-lattice analysis with the structures observed on the broad faces of the two types of α plate in a fundamental manner is a non-trivial task. On a general theory of precipitate morphology [15, 16], these faces should be those exhibiting the largest average inter-ledge spacing, particularly during the earlier stages of growth. The O-lattice analysis, however, yields only the geometry and spacings of the misfit dislocation arrays. A quantitative connection--if any in fact exists--between the misfit dislocation structure and the growth ledge structure (particularly the average inter-ledge spacing) has yet to be established. Comparison of the results of the present experiments with the O-lattice calculations summarized in Tables I and II indicates that this connection is not the obvious possibility of a proportionality between inter-dislocation and inter-ledge spacings. Thus, Table I suggests that either the second or the third {111} interface listed may correspond to the experimentally observed spacing of about 20 nm between misfit dislocations on a $\{111\}_\beta$ habit plane of *normal* α. Similarly, Table II indicates that either the third or the fourth interface listed in the $\{110\}_\beta$ category may be the calculated equivalent of the experimental $\{110\}_\beta$ habit plane with about a 35 nm inter-dislocation spacing on *black plates*. That the experimental spacings between dislocations are in both cases somewhat larger than those calculated is to be expected; the most common difference between "kinetic" and "equilibrium" interfacial structures is a too-wide inter-dislocation spacing experimentally observed [16]. Loss of the driving force for the acquisition of misfit dislocations is nearly complete by the time that most of the misfit dislocations which would be present at equilibrium have been secured; hence acquisition of the remaining dislocations is likely to be a rather lengthy process. That

Table I Calculated Burgers Vectors, Dislocation Spacings and Habit Planes for *Normal* α

b_1	b_1	d_1 nm.	d_2 nm.	θ degrees	$\{hkl\}_\beta$
a/2[111]	a/2[$\bar{1}$11]	198.8	198.8	3.3	
a/2[$\bar{1}$11]	a/2[$\bar{1}1\bar{1}$]	17.1	0.8	42.5	{111}
a/2[111]	a/2[$\bar{1}1\bar{1}$]	16.1	0.8	45.9	
a/2[$\bar{1}$11]	a/2[11$\bar{1}$]	32.9	2.4	20.6	
a/2[11$\bar{1}$]	a/2[$\bar{1}1\bar{1}$]	1.0	0.6	63.1	{110}
a/2[111]	a/2[11$\bar{1}$]	39.0	2.9	17.2	
a[010]	a[001]	1166.9	1166.9	0.6	
a/2[$\bar{1}1\bar{1}$]	a[010]	0.8	16.7	43.9	
a/2[11$\bar{1}$]	a[010]	2.6	35.2	19.2	{100}
a/2[$\bar{1}1\bar{1}$]	a[001]	0.8	16.5	44.5	
a/2[11$\bar{1}$]	a[001]	2.7	36.2	18.6	
a/2[111]	a[001]	479.1	479.5	1.4	
a/2[$\bar{1}$11]	a[010]	479.5	479.5	1.4	{122}
a/2[$\bar{1}$11]	a[001]	339.6	339.9	2.0	
a/2[111]	a[010]	339.6	339.9	2.0	

Table II Calculated Burgers Vectors, Dislocation Spacings and Habit Planes for *Black Plates*

b_1	b_1	d_1 nm.	d_2 nm.	θ degrees	$\{hkl\}_\beta$
a/2[111]	a/2[$\bar{1}$11]	6.3	6.3	17.1	{111}
a/2[$\bar{1}$11]	a/2[11$\bar{1}$]	6.5	2.7	16.7	
a/2[111]	a/2[11$\bar{1}$]	239.0	99.1	0.5	
a/2[111]	**a[001]**	**30.6**	**31.2**	**3.5**	**{110}**
a/2[$\bar{1}$11]	**a[010]**	**30.6**	**31.2**	**3.5**	
a[010]	a[001]	10.7	10.7	10.2	
a/2[$\bar{1}$11]	a/2[$\bar{1}$1$\bar{1}$]	2.3	0.6	52.4	
a/2[111]	a/2[$\bar{1}$1$\bar{1}$]	2.0	0.5	69.5	
a/2[111]	a[010]	7.9	8.0	13.7	{112}
a/2[$\bar{1}$11]	a[001]	7.9	8.0	13.7	
a/2[11$\bar{1}$]	a[001]	14.5	35.8	3.0	
a/2[$\bar{1}$1$\bar{1}$]	a[010]	0.6	2.3	55.9	
a/2[11$\bar{1}$]	a[010]	3.4	8.3	13.2	{113}
a/2[$\bar{1}$1$\bar{1}$]	a[001]	0.6	2.1	66.0	
a/2[11$\bar{1}$]	a/2[$\bar{1}$1$\bar{1}$]	0.8	0.5	69.1	{122}

the second array of misfit dislocations is not observed in either case is also to be anticipated from the calculations and experience. In the case of of *normal* α plates, the calculated inter-dislocation spacing of 0.8 nm is below the limit of resolution estimated to have been achieved in the present experiments, i.e., 1.5 to 2 nm., while in that of *black plates*, the calculated angle between misfit dislocation arrays, 3.5°, is so small that resolution of both arrays is not to be expected.

Table II shows that if the habit plane developed experimentally is that with the largest inter-dislocation spacing because this would yield the largest average inter-ledge spacing, then a $\{110\}_\beta$ habit plane should indeed have developed for *black plates*. However, this ought to have been the particular variant of $\{110\}_\beta$ in which the spacing between one array of dislocations was 239 nm and the other 99 nm (with only one array being visible because of the 0.5° angle between them), rather than the 35 nm actually observed. In the case of *normal* α, a {110} or a {122} habit plane would have been preferable on this basis to the {111} habit plane, actually operative, and even in the context of the {111} habit, a 199 nm inter-dislocation spacing, rather than the one with ~20nm should have been anticipated. Hence the simple hypothesis that misfit dislocation and ledge spacings are proportional is demonstrated to be unsatisfactory. This is, of course, just a part, though probably a central one, of the larger problem of the need for quantitative theories for the formation of growth ledges. As an ever larger proportion of interphase boundary structures turns out, with improved TEM instrumentation and operating technique, to be partially coherent [17, 18], this problem can only continue to "grow" in importance.

We may, however, conclude on a more hopeful, though also more empirical note by remarking that both the much lower ledge density and the wider spacing between misfit dislocations expected on the broad faces of "black plates" than on those of "normal α" because of the much higher perfection of "black plates" has been experimentally confirmed. In light of this discussion, however, the correlation of

a larger inter-ledge spacing with a larger inter-dislocation spacing on "black plates" vis a vis "normal α" must be regarded as fortuitous.

2.2. Identification of the Rejector Plate Mechanism During the Growth of Grain Boundary Alpha Allotriomorphs

This study was undertaken as part of a program to compare the nucleation, growth and overall kinetics of grain boundary allotriomorphs of proeutectoid α with those of the β --- α_m massive transformation in Ti-X alloys in order to ascertain the factors governing the appearance of these two alternative modes of transformation [3], The results secured were reported in last year's Interim Technical Report, with the exception of the following material, subsequently obtained, on the growth kinetics of proeutectoid α allotriomorphs.

Previous investigations have shown that when the matrix phase is a substitutional solid solution with an fcc crystal structure, transformation at reaction temperatures whose homologous temperature is less than ca. 0.9 that of the melting temperature for the alloy yield kinetics faster than those observed by means of volume diffusion directly toward the growing allotriomorphs [19, 20]. The deduction was made that growth proceeds by a "collector plate" mechanism. Solute diffuses toward the grain boundaries via volume diffusion through the matrix phase and thence along the grain boundaries to the allotriomorphs. Upon arriving at the allotriomorphs, some solute is deposited at the edges; the remainder diffuses through the partially disordered broad faces and deposits thereon. This mechanism yields a reasonable accounting for the observed growth kinetics and has now been quite widely accepted. An equivalent mechanism was subsequently invoked to explain the accelerated dissolution of grain boundary allotriomorphs in Al-Cu and Al-Ag alloys [21, 22].

No previous studies have been reported, however, of allotriomorph growth (or dissolution) kinetics in a substitutional binary alloy when the matrix has a bcc crystal

structure. Since the ratio of grain boundary to the volume diffusivity in bcc metals tends to be appreciably less than in fcc metals [22], the prediction was made that the collector plate mechanism would be less effective when the matrix is bcc [20]. The present investgation has provided an opportunity to test this prediction. Although the α phase precipitate is solute-poor rather than solute-rich, the "rejector plate" mechanism is simply the opposite of the "collector plate" one with excess solute now being rejected through the interphase boundary, thence through the grain boundaries and on into the matrix via volume diffusion.

Specimens of Ti-3.9 w/o Co and Ti-7.15 w/o Cr alloys were solution annealed for 20 min. at 1000°C in the form of sheet 80 micron thick. The grain boundaries in these specimens were essentially perpendicular to their broad faces. Hence the thickest and longest allotriomorph should be one of those first nucleated and also one sectioned equatorially by the plane of polish, established parallel to the specimen broad faces [23]. Fig. 4 shows the plots of maximum half-length (L/2) and maximum half-width (S/2) vs. $(\text{reaction time})^{1/2}$ for both alloys at allreaction temperatures employed. The slopes of these plots are the parabolic rate constants for lengthening, β, and for thicking, α, respectively.

When volume diffusion controlled, the growth kinetics of grain boundary allotriomorphs are customarily approximated [20, 24] as those of oblate ellipsoids of revolution. The solution to this diffusion problem is a specialized form of the one developed by Ham [25] and by Horvay and Cahn [26]. However, this solution includes an integral which Horvay and Cahn [27] evaluate by means of one series expansion for low aspect ratios and another expansion for aspect ratios near unity. Recently, it was shown that the integral could be evaluated and expressed in terms of the familiar error function [9]. The parabolic rate constants for thickening, α, and for lengthening, β, are written as [9]:

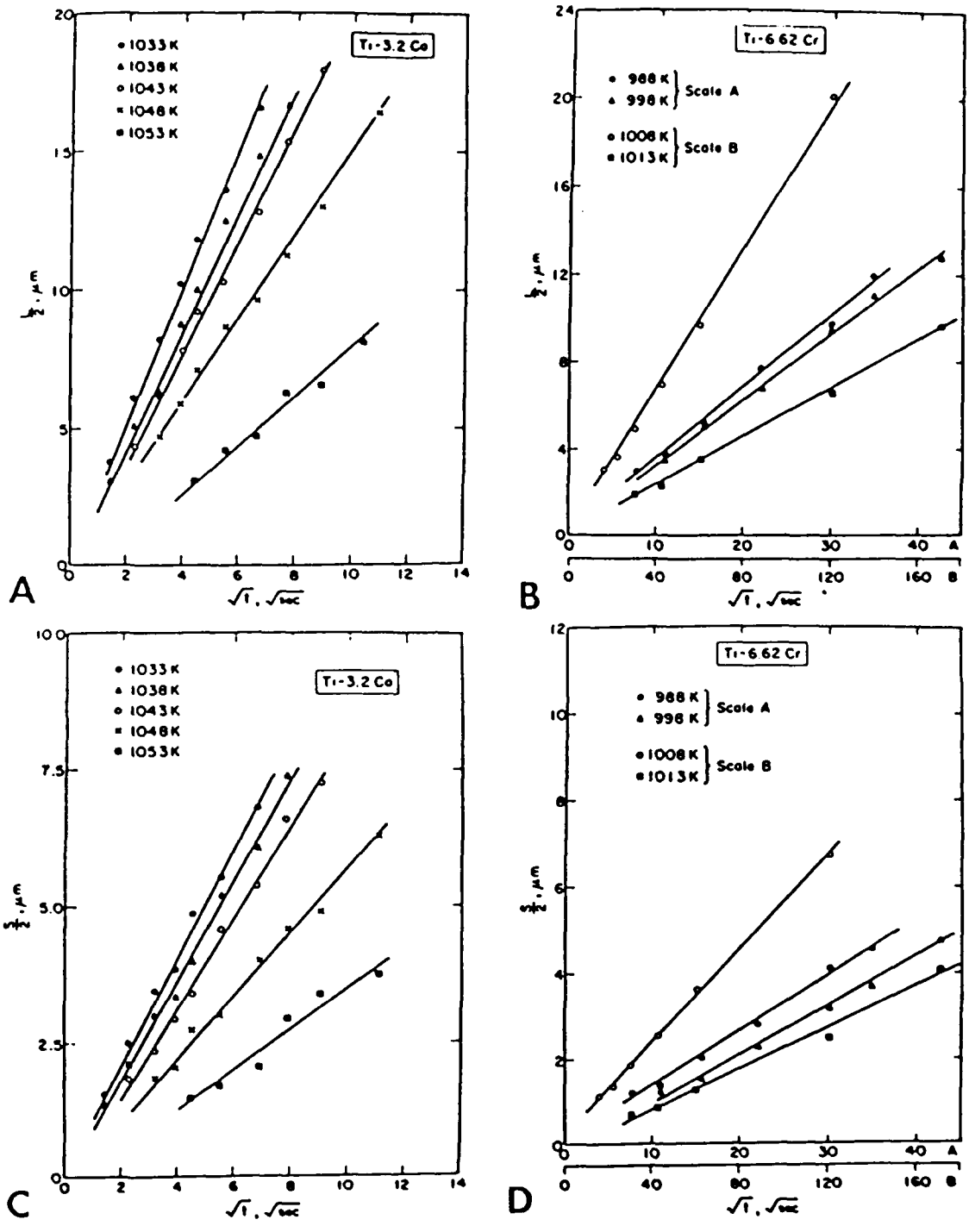

Figure 4: Plots of half-length, L/2, of grain boundary allotriomorphs versus $t^{1/2}$, for (a) Ti-3.2 at% Co and (b) Ti-6.6 at% Cr. (c) and (d) are plots of half-thickness, S/2, versus $t^{1/2}$, for the two alloys, respectively

$$\alpha = 2R\sqrt{\Omega D} \tag{1}$$

$$\beta = 2\sqrt{\Omega D} \tag{2}$$

where R is the aspect ratio of the oblate ellipsoid, D is the volume diffusivity and Ω is a parameter denoting the precipitate:matrix interface and can be obtained by solving the transcendental equation [9]:

$$2e^{\Omega}\,\Omega^{3/2}\left[\frac{e^{-\Omega}}{\Omega^{1/2}} - \sqrt{\pi}\;erfc\{\sqrt{\Omega}\}\right] = \frac{X_{\beta}^{\beta\alpha} - X_{\beta}}{X_{\beta}^{\beta\alpha} - X_{\alpha}^{\alpha\beta}} \tag{3}$$

where $X_{\beta}^{\beta\alpha}$ and $X_{\alpha}^{\alpha\beta}$ are the atom fractions of solute in β at the $\beta/(\alpha + \beta)$ phase boundary and in α at the $\alpha/(\beta + \alpha)$ phase boundary at a given temperature and X_{β} is the alloy composition.

The theoretically calculated and experimentally determined parabolic rate constants for the two alloys used in this study are compared in Fig. 5. The experimental parabolic rate constants are seen to lie increasingly above those calculated with decreasing reaction temperature. This result strongly suggests that growth of α allotriomorphs is significantly aided by the "rejector plate" mechanism. This deduction is supported by calculating an apparent diffusivity, D_{app}, from Eqns. (1) - (3) through substitution of the experimental parabolic rate constants. Comparison with the independently obtained volume diffusivities, D_v, in Table III shows that the ratio $\frac{D_{app}}{D_v}$ increases with decreasing temperature. This is just the behavior previously reported for the growth kinetics of grain boundary θ allotriomorphs in Al-4 wt% Cu [20, 19].

In order to compare in approximate fashion the effectiveness of interfacial diffusion-aided growth of grain boundary allotriomorphs in the present bcc alloys with that in fcc alloys, the approach of Goldman et al [20] is employed. Using the

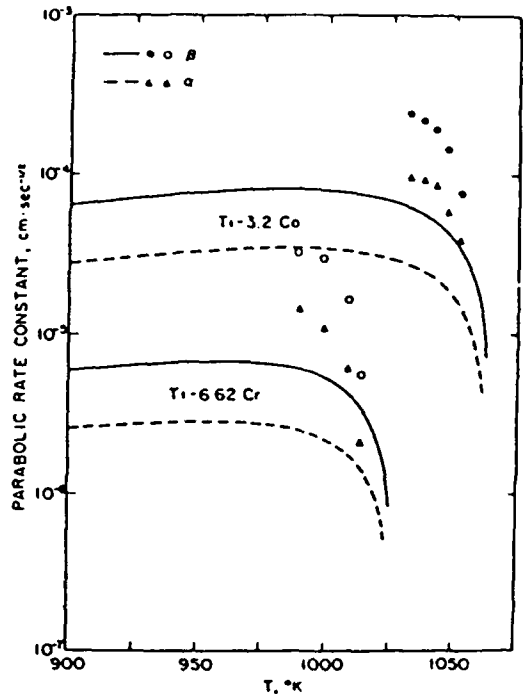

Figure 5: Parabolic rate constants for lengthening, β, shown by circles and for thickening, α shown by triangles as a function of isothermal reaction temperature, T, for Ti-3.2 at% Co (filled symbols) and for Ti-6.6 at% Cr (open symbols). The lines (continuous for β and dashed for α) were calculated from Eqns. (1) - (3).

Table 2-1: Calculated Apparent Diffusivities During Allotriomorph Growth

Ti-3.2 at% Co			Ti-6.62 at% Cr		
T in K	$\frac{D_{app}}{D_v}$(*)	$\frac{D_{app}}{D_v}$ (**)	T in K	$\frac{D_{app}}{D_v}$(*)	$\frac{D_{app}}{D_v}$ (**)
1033	14.8	15.7	988	31.0	36.2
1038	14.6	16.7	998	31.6	26.5
1043	14.8	17.2	1008	14.9	12.7
1048	10.7	10.5	1013	2.5	2.2
1053	4.9	7.6			

(*) -- calculated from lengthening kinetics

(**) -- calculated from thickening kinetics

solidus temperature at the bulk alloy composition as T_m, and the average temperature of the narrow temperature ranges available for growth kinetics measurements as T, Table III shows that in Ti-6.6 at% Cr at $\frac{T}{T_m} = 0.53$, $\frac{D_{app}}{D_v} \approx 32$, and in Ti-3.2 at% Co, at $\frac{T}{T_m} = 0.58$, $\frac{D_{app}}{D_v} \approx 15$. Referring to Fig. 7 of Goldman et al [20], $\frac{D_{app}}{D_v}$ for Al-4 wt% Cu (where the matrix is fcc α phase) at $\frac{T}{T_m} = 0.55$ is ≈ 700. Thus the collector/rejector plate mechanism appears to be less effective when the matrix has a bcc structure than when it is fcc at a given homologous temperature, doubtless because $\frac{D_b}{D_v}$ (where D_b is the grain boundary diffusivity) is smaller in bcc metals [28, 29] as a consequence of the less dense packing in the bcc lattice.

Analyses have been developed for obtaining grain boundary and interphase boundary diffusivities from growth kinetics when the collector/rejector plate mechanism is the dominant contributor to mass transport [19, 20, 30]. However, these diffusivities appear in combination with the solute concentration within the

interfaces in the analyses. Different estimates of these solute concentrations can lead to drastically different interfacial diffusivities and activation energies for these diffusivities. Since this problem has yet to be resolved either experimentally or theoretically, calculation of grain boundary and interphase boundary diffusivities attending the growth of α allotriomorphs by the rejector plate mechanism is foregone for the present. The results reported for $\frac{D_{app}}{D_v}$ have accomplished our objective of securing at least an initial comparison of the efficacy of the collector/rejector plate mechanism in a bcc matrix with that in an fcc matrix.

2.3. Influence of Beta Grain Size upon Formation of Widmanstatten Alpha Plates in Ti-Cr Alloys

2.3.1. Introduction

This investigation is the Ph.D. thesis research of Miss Amber Dalley. She is supported by a Fellowship provided by the CMU Department of Metallurgical Engineering and Materials Science; our AFOSR grant provides her equipment and supplies.

That reducing the austenite grain size tends to inhibit formation of Widmanstatten ferrite plates in steel has been recognized for about a century. There do not appear, however, to be any explicit published recognitions that this effect might also influence the development of proeutectoid α plates in hypoeutectoid Ti-base alloys. Froes and co-workers [31] have demonstrated that fatigue properties of titanium alloys are significantly improved when Widmanstatten morphologies of proeutectoid α are replaced by grain boundary allotriomorphs. In a collaborative paper shortly to be prepared with Dr. Froes and his colleagues it will be pointed out, upon the basis of research now being conducted in a Ti-6% Al- 4% V aerospace alloy, that reducing β grain size does indeed tend to cause replacement of the Widmanstatten α morphologies by that of allotriomorphs. In part, the present investigation is intended to examine this correlation in more quantitative detail. However, it is also expected

that this study will permit "leapfrogging" those reported in steel and permit a much more fundamental investigation to be conducted of both the evolution of α sideplates from grain boundary allotriomorphs and of the effects of reducing β grain size upon this process. The reason for the anticipated advance is that in steel the austenite which remains untransformed at the transformation temperature is usually converted more or less completely to martensite during quenching to room temperature. This process prevents observation of the structure of austenite:ferrite boundaries via TEM at room temperature. In Ti-X alloys, however, proper selection of an alloy system and a composition range within that system permits complete suppression to the martensite transformation to be accomplished with little difficulty. The Ti-7.15% Cr alloy being used as the initial one in this investigation shows no trace of martensite even when directly quenched from the β to room temperature.

We thus plan to study sideplate evolution from α allotriomorphs by examining the misfit dislocation, and especially, the growth ledge structure of protuberances on the allotriomorphs and their development into sideplates. An attempt will then be made to interpret these obsevations on the basis of the Mullins-Sekerka theory of morphological instability [32, 33], and especially in terms of the modification currently being made in the theory to accomodate growth anisotropy [34].

2.3.2. Rapid Solidification Processing Studies

The key to making the grain size component of this program viable is achieving large and controlled reductions in β grain size. Unlike steel, Ti-base alloys contain only small concentrations of grain growth-inhibiting inclusions. Given also the high diffusivities characteristic of the β phase, it is normally not possible to heat treat so as to obtain β grain sizes which are not very large. Froes and his colleagues have done so in alloys where porosity or inclusions remaining from the alloy preparation process inhibit grain growth; for a fundamental study such as the present one, however, this type of approach is not desirable. However, during the first visit which the P.I. paid to Dr. Froes's laboratories, he was shown β titanium with a grain size of

only 0.1 um. This feat was accomplished by means of rapid solidification. Hence the initial experimental efforts made on this program have been directed toward reproducing this important result. We are also seeking to ensure that the rapid solidification processing is conducted under conditions which minimize contamination of our Ti-Cr alloy by oxygen, nitrogen and other interstitial (and of course also substitutional) impurities. Finally, we seek to validate the utility of the small β grain sizes obtained by ascertaining whether or not grain boundary allotriomorphs can be precipitated in these specimens, thereby pinning the β grain boundaries, before significant grain growth can occur in the β phase.

Three different modes of rapid solidification processing (RSP) have been utilized. Each was performed for us at another laboratory. These methods, and the results achieved from them, are the following:

(i) Pendant drop method (Wright-Patterson AFB--Dr. S. Krishnamurthy)

Beta grain sizes ranged from 15 to more than 200 um. These large grain sizes evidently developed when the rapidly solidified ribbon broke away from the rotating heat-extraction cylinder upon which the "splats" were formed. Slow cooling in vacuo then appears to have permitted grain growth to have occurred from may well have been a small initial grain size. Microstructural evidence was found appreciable dissolution of interstitial ompurities during processing.

(ii) Hammer-and-anvil method (Oak Ridge National Laboratory--Dr. F.A. Kroger)

Splats produced by this method were duplex in nature. The larger proportion of their volume had a β grain size of about 30 um; the balance was characterized by a grain size of about 1 um. Evidence for interstitial contamination---again in the form of precipitation, presumably of proeutectoid α, at sub-boundaries prior to the onset of significant allotriomorph formation at β grain boundaries, was again observed. This effect of oxygen contamination upon transformation processes was identified more than 30 years ago by Delazaro and Rostoker in Ti-11% Mo alloys [35].

(iii) Vapor Phase Quenching (IBM T.J. Watson Research Center--Dr. D.A. Smith)

This technique produced a combination of amorphous alloy and β grain sizes so small that they could not be measured with ordinary TEM techniques. The foils were very fragile and thus difficult to manipulate after preparation.

The splats produced by the hammer-and- anvil technique were judged sufficiently promising so that they were heat treated in order to permit a preliminary evaluation of β grain size stability during heat treatments designed to produce proeutectoid α formation. Fig. 6a shows the β grain size in the fine-grained region of an ORN1 splat, as received. Fig. 6b indicates the β grain size after reaction for 20 min. at 750°C. The β grain size is seen to have increased 2-3X. Grain Size is still sufficiently small to be useful, but inhibition of the grain growth process by partially pre-thinning specimens prior to heat treatment and the use of lower reaction temperatures would clearly be desirable.

Fig. 6b also indicates that the specimen was contaminated by interstitials, presumably during RSP. Precipitation at intragranular dislocations is visible in the coarser β grains. Additionally, though, the grain boundary allotriomorphs have a peculiar appearance. They look like the "black plate" version of allotriomorphs, i.e., dark smooth and thin when viewed with optical microscopy. Fig. 7, taken at a higher magnification, more clearly shows the well formed "black plates" in the interiors of the β grains and their allotriomorphic counterparts. This result indicates that interstitial contamination has raised the transition temperature from "normal α" to "black plates" by at least 130°C! Clearly, this is highly undesirable and indicates that a significant improvement in the RSP process will be needed in order to secure usable specimens. On the other hand, the adventitious observation of apparent "black plate allotriomorphs" provides a valuable addition to the next research program to be described.

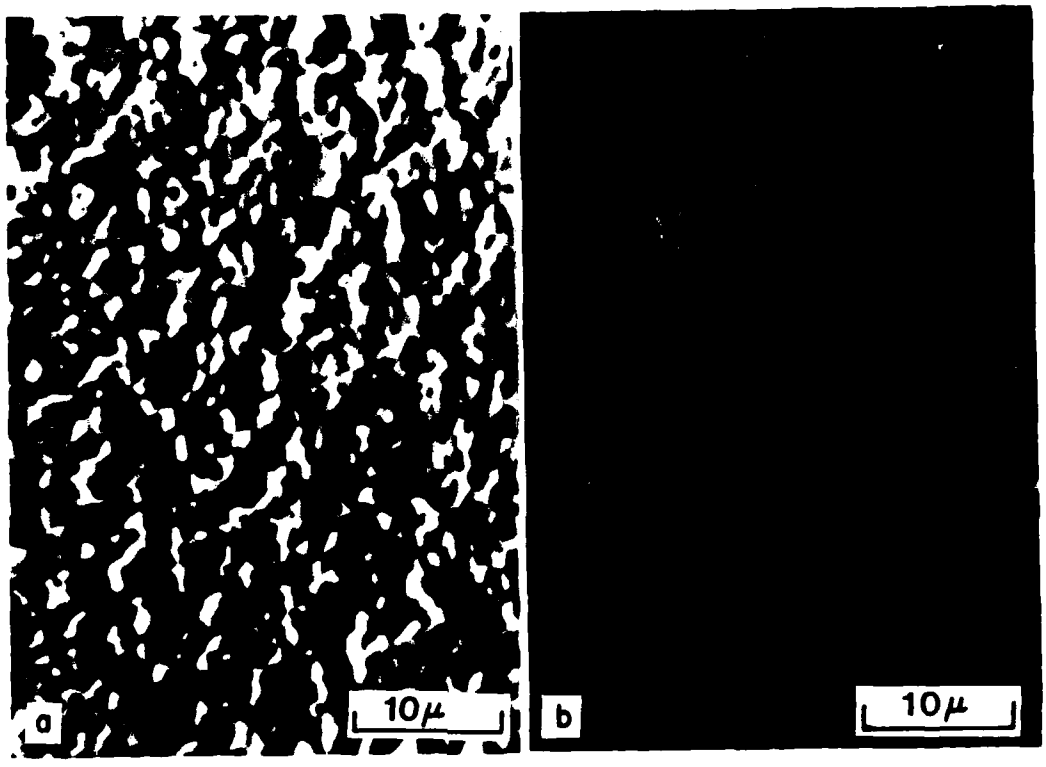

Figure 6: Optical micrographs ofsplat-quenched Ti-6.6a/o Cr alloy demonstrating the vriation of β grain size during isothermal heat treatment. A) microstructure of an ORN1 splat, as received, showing fine grain size of β phase; B) microstructure after reaction at 750°C for 20 min. The β grain sizes are increased ca. 2 - 3 times. Etched in 20% HF, 20% HNO_3,and 60% glycerin.

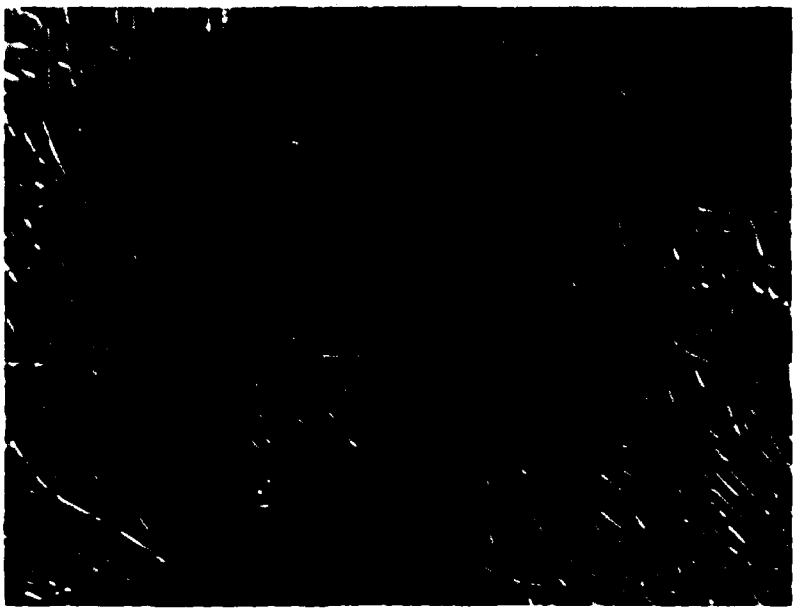

Figure 7: Higher magnified optical micrograph of Fig. b, showing the black plates in the interiors of the β grains. Etched in 20% HF, 20% HNO_3, and 60% glycerin.

2.3.3. Preliminary Observations on Sideplate Evolution from Grain Boundary Allotriomorphs

Although these observations are preliminary almost to the point of being casual, and were made while Miss Dalley was acquiring expertise with TEM, their importance strongly indicates that the experimental feasibility of the planned investigation of sideplate evolution from grain boundary allotriomorphs is well on its way to being established. Fig. 8a shows three grain boundary α allotriomorphs at a β grain boundary in our Ti-7.15% Cr alloy. Note that all have similar shapes and that (usually faint) signs of interphase boundary structure such as suggest the presence of partial coherence are present at all exposed orientations on both sides of the β grain boundary. Further, on the left hand side of each allotriomorph, a protuberance is starting to develop. In the left-most allotriomorph, this has already developed into the beginnings of a sideplate. Hence it would appear that many more experimental observations, accompanied by extensive tilting of the foils, and the use of high magnifications, will permit us to examine fully the various stages in the development of sideplates and of the interphase boundary structure at and adjacent to the protuberances which will later become sideplates.

Fig. 9 samples an unexpected observation: the three sideplates which are extensively in contact with the grain boundary allotriomorphs appear to have a different orientation than the allotriomorphs in at least two cases and to have been sympathetically nucleated at an interphase boundary of the allotriomorphs in all three. Close observation of the areas which the sideplates are in contact with the allotriomorphs are thus much more suggestive of separate nucleation and growth rather than of evolution from protuberance. Evidently, sympathetic nucleation can play a significant role in sideplate formation in this alloy, and by implication, in other Ti-X systems as well. Perhaps this observation is not so surprising if one recalls that sympathetic nucleation has been known to play a major role in the development of proeutectoid α plates for nearly 30 years [36]. An extensive theoretical

Figure 8: BF elecron micrographs of Ti-6.6 a/o Cr, rapidly solidfied by pendant drop melt method, isothermally reacted at 750°C for 10 min: a) Formation of grain boundary α allotriomorphs at a β grain boundary; b) Protuberance of sideplates at grain boundary allotriomorphs. Partial coherence exists at all interphase boundaries.

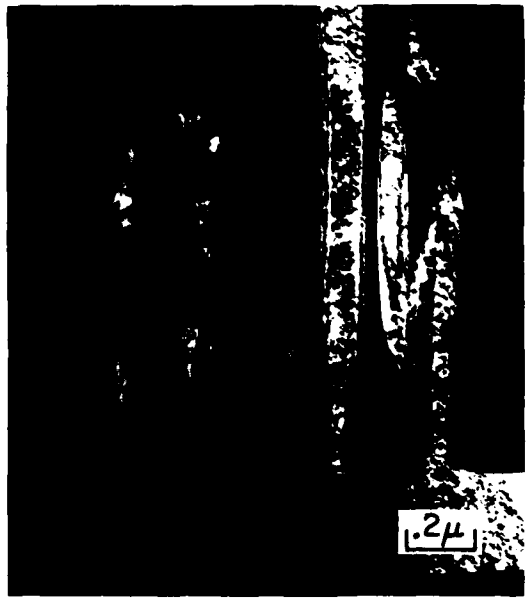

Figure 9: DF micrograph of Ti-6.6 a/o Cr, rapidly solidfied by pendant drop melt method, isothermally reacted at 750°C for 10 min, showing the evolution of sideplates from the grain boundary α allotriomorph by sympathetic nucleation.

(crystallography and kinetics) and experimental (TEM) analysis of sympathetic nucleation in Ti-X, and especially Ti-Cr alloys, was made during Dr. Menon's Ph.D. thesis and should soon appear in print [5]. This investigation will provide guidelines for more quantitative studies of sideplate formation by sympathetic nucleation in Ti-Cr alloys.

Durng the coming year, we hope to secure good data on the influence of β grain size on the highest temperature at which sideplates can form (the W_s temperature) in the Ti-7.15% Cr alloy. We also plan to place the foregoing observations on sideplate evolution upon a firmer basis, with particular attention being paid to the variation in inter-ledge spacing at, in the vicinity of, and remote from protuberance in allotriomorphs. One should perhaps expect that protuberances will evolve where this spacing passes through a minimum. If this does obtain experimentally, then one may ask: are the locations of the minima determined by chance, by the presence of certain configurations of facets forming relative small dihedral angles where they meet, by diffusion distance and capillarity considerations a la Mullins-Sekerka [32, 33], by some combination of these factors---or by others still unknown? We do indeed "have our work cut out for us", but unlike the situation in Fe-C-base alloys, the survival of the untransformed β as such down to room temperature and the reasonable kinetics of α formation should enable us to do some constructive things about this task.

2.4. Crystallography and Interfacial Structure of Grain Boundary Alpha Allotriomorphs and of Compound Precipitation at These Allotriomorphs

This program will constitute the Ph.D. thesis research of Mr. Tadashi Furuhara, who came to us from Kyoto University, Japan, where he did his M.S. research with Dr. Minoru Umemoto and Prof. Imao Tamura. The P.I. was the guest of Prof. Tamura when he visited Japan for five weeks, 2 and 1/2 years ago, under the auspicies of the Japan Society for the Promotion of Science. Mr. Furuhara is presently supported

by the CMU Department of Metallurgical Engineering & Materials Science and is spending most of his time on coursework and on learning TEM theory and techniques. When Mr. Hwack Joo Lee completes his research on the bainite reaction (described in the next section), Mr. Furuhara will be supported by this AFOSR Grant.

The primary goals of this program are to examine the structure of the interphase boundaries between grain boundary allotriomorphs of proeutectoid α nd both β grains forming the boundaries at which the allotriomorphs are formed. Except for a few scattered observations, no investigation of this type appears to have been reported so far in any alloy system. While we have long been considered the interphase boundary structure of grain boundary allotriomorphs to be primarily disordered in character [15], theoretical considerations on nucleation strongly indicate that the structure of these boundaries ought to be primarily coherent during nucleation and partially coherent during growth [37, 17]. Figs. 8-10 in this report provide further support for this view. As will shortly be noted, it is the prevailing opinion in this research area that a grain boundary allotriomorph will enjoy a low energy lattice orientation relationship with respect to only one of the matrix grains forming the boundary at which the allotriomorph nucleated. Widmanstatten sideplates have developed into only one β grain from the allotriomorphs in Fig. 10; presumably the usual Burgers orientation relationship obtains between the allotriomorphs and this grain. However, probable growth ledges can be discerned at the rather smoothly curved boundaries between the allotriomorphs and the "other" β grain, in support of our deduction of orientation relationships capable of producing low energy interphase boundaries with respect to both β grains [17, 38].

The most thorough investigation so far made of the crystallography of grain boundary allotriomorph precipitation is that of Park and Ardell [39]. They studied precipitation of the hcp η phase in the complex commercial Al-base alloy known as 7075. They found that at a given grain boundary one particular variant of the lattice

Figure 10: DF micrograph of Ti-6.6 a/o Cr, rapidly solidfied by pendant drop melt method, isothermally reacted at 750°C for 10 min, showing the development of Widmanstatten sideplates from the grain boundary α allotriomorph.

orientation relationships prevails with respect to one of the bounding matrix grains. When the principal habit plane operative is nearly parallel to the grain boundary plane, nucleation kinetics appear to be particularly rapid. These considerations were forecast sometime ago by Lee and Aaronson [40, 41], using a simplified model of the critical nucleus, wherein only low energy habit plane is present; at all other boundary orientations the interfaces were taken to be disordered. No attempt was made, however, to examine the possibilities for low energy orientation relationships with respect to the "other" matrix grain. The only systematic attempt to do this so far reported is that of Plichta and Aaronson [42] (done with the support of this grant) on the bcc β--- hcp ξ_m massive transformation in a Ag-26a/o Al alloy. They observed the Burgers orientation relationship with respect to one β grain and some other relationship with respect to the adjacent β grain or grains (the latter when nucleation took place at a grain edge instead of at a grain face). Use of O-lattice analysis revealed that some of the orientation relationships with respect to the "other" β grain could produce low energy interphase boundaries; others did not appear to be of this type. Invariably, however, facets appeared on the all allotriomorphs as they grew in <u>both</u> β grains. A less complete earlier study by King and Bell [43] on the proeutectoid ferrite reaction in an Fe-C alloy, performed with the Kossel micro-diffraction, back-reflection technique yielded similar crystallographic and morphological results, though no O-lattice analyses were attempted.

In the present investigation, we shall consider orientation relationships and habit planes as secondary characteristics of allotriomorph crystallography and interphase boundary structure. Instead, TEM studies will be conducted of the interphase boundary structure of <u>both</u> broad faces of allotriomorphs, i.e., the face between the allotriomorph and the β grain with which it does have a Burgers relationship, and that with the β grain in which it does not. Both the misfit dislocation structure and the growth ledge structure will be characterized. Efforts will be made to connect the details of non-Burgers orientation relationship with the crystallographic details of the

misorientation of the β grains forming the grain boundary and the angle of the grain boundary plane with respect to the symmetry plane of the grain boundary. On the basis of Fig. 8-10, we do now expect to see partially coherent structures on all of allotriomorphs studied. If feasible, we will attempt to correlate interphase boundary structure (particularly, the average spacing between growth ledges) with growth kinetics through measurements of the relative dimensions achieved by the allotriomorphs. Interpretation will be based upon interactive consideration of the crystallographic data obtained and the critical nucleus shape.

The second portion of this investigation would examine the precipitation of $TiCr_2$ at the allotriomorphs with respect to correlating favored sites for such precipitation with the interphase boundary structure of the allotriomorph. It has been seriously proposed that alloy carbides can precipitate on moving, disordered interphase boundaries of ferrite allotriomorphs in Fe-C-X alloys [44], despite strong theorectical arguments against the kinetic feasibility of this process [45]. The present study will transfer this argument to Ti-Cr, where observation of the interphase boundary structure makes decisive resolution of the argument a feasible proportion. Mr. Lee's thesis research has suggested that intermetallic compound precipitation occurs preferentially on misfit dislocations rather than on growth ledges. Since one might reasonably anticipate that interphase boundaries formed between non-Burgers related α:β couples would have a higher density of misfit dislocations in order to compensate for the poorer matching anticipated across this interphase boundary, a higher nucleation rate of $TiCr_2$ might be anticipated at the non-Burgers broad face of grain boundary α allotriomorphs.

It is anticipated that the results of this investigation will have widespread applicability to directly analogous transformation processes, particularly the bainite reaction, in steel, and to related processes, e.g., the precipitation of the n+1'st transition phase at the interphase boundaries of the n'th transition phase, in Al-base and other age-hardening types of alloy system.

3. THE BAINITE REACTION

3.1. Introduction

This program constitutes the Ph.D. thesis research of Mr. Hwack Joo Lee. Completion is presently anticipated by the end of February. During the past report year, the experimental work performed on this program has been primarily in the area of gathering quantitative data on the heights and spacings of growth ledges, the tilt angle of surface relief effcts associated with the formation of proeutectoid α plates at a free surface and lattice orientationships. With the exception of the surface relief data, this information is primarily intended to make quantitative use of the analysis now to be presented.

This analysis was "nucleated" by the nearly simultaneous observation of the interfacial structure of the edges of pearlite colonies in an Fe-0.8% C-12% Mn alloy (in which untransformed austenite is fully retained even in thin foils) by Hackney and Shiflet [46, 47] and of bainite structures in a hypereutectoid Ti-25% Cr alloy during the present investigation. The product phases in steel were ferrite and cementite while those in the Ti-Cr alloy were α and $TiCr_2$. For the sake of generality, we shall term the matrix phase in these eutectoid reactions γ and the two product phases α and β, with α being understood to be solute-poor and β to be the solute-rich intermetallic compound. In pearlite, Hackney and Shiflet found some direct and more indirect evidence that both α:γ and β:γ interfaces are partially coherent. Both phases were demonstrated (via hot stage TEM) to grow by means of the ledge mechanism. However, they observed that the growth ledges are <u>shared</u> by the α and the β phases; hence the inter-ledge spacing and presumably also the ledge height at α:γ interfaces in the pearlite studies are the same as those on β:γ interfaces. No explanation has as yet been found for the crystallographic feasibility of this remarkable observation, though it appears to be factually incontestable. In the hypereutectoid Ti-Cr alloy (and also in hypoeutectoid Ti-Fe alloy), Mr. Lee has

repeatedly shown directly that both α:γ and β:γ interfaces contain misfit dislocations. Growth ledges are found on both types of interface as shown in Fig. 11. The spacing between growth ledges, the height of the ledges and also the growth direction of the ledges are different on the two types of interphase boundary. These, then, are the new experimental facts with which the following analysis attempts to deal.

3.2. Treatment of the Growth Kinetics of Pearlite and Bainite

The present analyses hew closely to the Fick's First Law treatments for the edgewise growth of pearlite published by Hillert [48] in 1972. His earlier [49] Fick's Second Law-based analyses yield nearly the same results, as expected in growth situations closely approximating steady state; hence for the sake of simplicity we utilize the model provided by the simpler treatment. Two important differences will, however, be introduced. Growth will now be considered to occur solely by the ledge mechanism. Hence Hillert-type equations will be modified in the style of Cahn, Hillig and Sears [50] and Jones and Trivedi [51]. The second modification is that of the growth of the two product phases produced by eutectoid decomposition will be decoupled. This will be seen to result directly from introduction of the ledge mechanism.

In the following considerations, when one product phase forms more voluminously and grows more rapidly than the other, let this phase be α unless otherwise specified. Assume that initially both α and β crystals are in contact with the γ matrix and that they appear alternately. Finally, ignore effects arising from variations in molar volume with solute concentration or differences in molar volume amongst the phases involved.

The assumption is first made that all mass transport takes place by volume diffusion through the γ matrix. The flux of solute away from an α crystal (toward one adjacent β crystal) may thus be approximated on the Zener-Hillert approach as:

a

b

Figure 11: a) BF micrograph illustrating the interfacial structures at the eutectoid alpha:beta interface in Ti-25w/o Cr alloy, beta solution treated and isothermally reacted at 635°C for 3 hours. The growth ledges are spaced ca. 210 nm apart with height 25 nm. The misfit dislocations are spaced 20 nm apart between the growth ledges; b) Df micrograph showing the interfacial structures at the eutectoid $TiCr^2$:beta intefaces in the same specimen. The growth ledges are spaced ca. 30 nm apart as arrows indicated.

$$J_1 = -A D_v \left(\frac{\partial x}{\partial S}\right)$$
$$\simeq \frac{l S_\alpha h_\alpha}{\lambda_\alpha} D_v \frac{(x_\gamma^{\gamma\alpha} - x_\gamma^{\gamma\beta})(1 - S_o/S)}{(S_\alpha/2)} \tag{4}$$

where l = an indeterminate distance along the α:γ boundary perpendicular to the diffusion direction, h_α = height of growth ledges on α:γ interfaces, λ_α = average spacing between these ledges , S_α = average width of α crystals, D_v = volume interdiffusity in γ, S = spacing between midplanes of adjacent α and β crystals, S_o = minimum S, at which all volume free energy change is consumed as α:β interfacial energy and $x_\gamma^{\gamma\alpha}$ and $x_\gamma^{\gamma\beta}$ = atom fractions of solute in γ at $\gamma/(\alpha+\gamma)$ and at $\gamma/(\beta+\gamma)$ boundaries, respectively. The flux of solute displaced into γ by the growth of an α crystal, J_2 = dm/dt, is given by:

$$J_2 = \frac{dm}{dt} = \frac{dm}{dv}\frac{dv}{dt} = (x_\gamma - x_\alpha^{\alpha\beta}) l S_\alpha G_\alpha \tag{5}$$

where v = volume of α added by growth through a normal distance ds = lS_αds, G_α = rate of growth of α = ds/dt and x_γ = atom fraction of solute in γ prior to transformation. Equating the fluxes described by Eqns. (4) and (5) and noting that the volume fraction of α, $f_\alpha = S_\alpha/S$ when the equilibrium proportions of α and β are formed:

$$G_\alpha = \frac{2 D_v h_\alpha (x_\gamma^{\gamma\alpha} - x_\gamma^{\gamma\beta})(1 - S_o/S)}{f_\alpha \lambda_\alpha S (x_\gamma - x_\alpha^{\alpha\beta})} \tag{6}$$

Applying Zener's [52] maximum growth rate hypothesis to the interlamellar spacing, i.e., taking $\partial G_\alpha/\partial S = 0$, for which important new justification has been provided by Trivedi [53] in situations equivalent to the present one, yields:

$$G_\alpha = \frac{D_v h_\alpha (x_\gamma^{\gamma\alpha} - x_\gamma^{\gamma\beta})}{f_\alpha \lambda_\alpha S (x_\gamma - x_\alpha^{\alpha\beta})} \tag{7}$$

Following the same type of procedure, the growth rate of β lamellae, G_β, is:

$$G_\beta = \frac{D_v h_\beta (x_\gamma{}^{\gamma\alpha} - x_\gamma{}^{\gamma\beta})}{f_\beta \lambda_\beta S (x_\beta{}^{\beta\alpha} - x_\gamma)} \tag{8}$$

In the case of pearlite, $G_\alpha = G_\beta = G$, the overall edgewise growth rate of pearlite. Hence:

$$\frac{h_\alpha}{f_\alpha \lambda_\alpha (x_\gamma - x_\alpha{}^{\alpha\beta})} = \frac{h_\beta}{f_\beta \lambda_\beta (x_\beta{}^{\beta\alpha} - x_\gamma)} \tag{9}$$

On the assumption of equilibrium fraction of the two precipitate phases:

$$\frac{f_\alpha}{f_\beta} = \frac{(x_\beta{}^{\beta\alpha} - x_\gamma)}{(x_\gamma - x_\alpha{}^{\alpha\beta})} \tag{10}$$

Substituting this relationship into Eq.(9):

$$\frac{h_\alpha}{\lambda_\alpha} = \frac{h_\beta}{\lambda_\beta} \tag{11}$$

Hence on the ledge mechanism,

$$G_v = \frac{D_v h (x_\gamma{}^{\gamma\alpha} - x_\gamma{}^{\gamma\beta})}{f_\alpha f_\beta \lambda S (x_\beta{}^{\alpha\beta} - x_\alpha{}^{\alpha\beta})} \tag{12}$$

for pearlite, where $h_\alpha/\lambda_\alpha = h_\beta/\lambda_\beta = h/\lambda$.

Similarly, when $G_\alpha \neq G_\beta$, it follows that:

$$h_\alpha/\lambda_\alpha \neq h_\beta/\lambda_\beta \tag{13}$$

Under this circumstance, one product phase, previously designated as α, grows faster than the other, i.e., β, more or less inevitably surrounding individual β crystals and terminating their direct access to γ. Local supersaturation of γ with respect to β nucleation thus develops, and re-nucleation of β at α:γ boundaries (presumably on

stationary portions thereof, i.e., on the terraces of ledges [54, 45]) must eventually occur. This cycle then repeats. A microstructure consisting of a dispersion of β precipitates within α thus develops. Hence the mechanism of the bainite reaction proposed by Hultgren [55] in 1947 is recovered. Therefore Eq. (11) describes the pearlite reaction and Eq. (13) leads to the bainite reaction.

Note that in the absence of the ledge mechanism, application of Eq.(10) makes Eqs. (7) and (8) equal, i.e., $G_\alpha = G_\beta = G$. Thus, as described by Hillert [56], α and β can indeed "learn to grow together" with much mutual kinetic advantage. In the presence of the ledge mechanism, however, pearlite can only form when the stringent condition of Eq.(11) is exactly fulfilled. When it is not, i.e., the inequality of Eq. (13) is satisfied, bainite inevitably develops. Given the erratic nature of the ledge mechanism as observed during a variety of diffusional phase transformations [57, 58], the "simple and exact" solution to the question of why pearlite appears to occur so much more readily than bainite during eutectoid decomposition in the broad range of alloy systems so far examined is that the Hackney-Shiflet [46] mechanism of shared ledges of equal height must be widely operative. Whether or not this hypothesis is correct, however, can only be answered by future experiments.

The same basic results, e.g., Eqns. (11) and (13), are now shown to obtain when all mass transport takes place by boundary-diffusion control. The flux of solute away from an α crystal is:

$$J_1 = \frac{\delta h_\alpha / D_b (x_\gamma^{\gamma\alpha} - x_\gamma^{\gamma\beta})(1 - S_o/S) K}{\lambda_\alpha \quad S^\alpha/2} \tag{14}$$

where δ = thickness of an interphase boundary and K = ratio of the solute concentration in α (or β) to that in the α:γ (or β:γ) boundary. The corresponding flux of solute displaced by growth of α is again given by Eq. (5). Equating these two fluxes:

$$G_\alpha = \frac{2 D_b \delta h_\alpha (x_\gamma^{\gamma\alpha} - x_\gamma^{\gamma\beta})(1 - S_o/S) K}{f_\alpha \lambda_\alpha S^2 (x_\gamma - x_\alpha^{\alpha\gamma})}$$

$$= \frac{2 D_b \delta h_\alpha (x_\gamma^{\gamma\alpha} - x_\gamma^{\gamma\beta})(1 - S_o/S) K}{f_\alpha f_\beta \lambda_\alpha S^2 (x_\beta^{\beta\alpha} - x_\alpha^{\alpha\beta})} \qquad (15)$$

With Hillert [48], $\partial G_\alpha / \partial S = 0$, when $S = (3/2)S_o$. Hence:

$$G_\alpha = \frac{2 D_b \delta h_\alpha (x_\gamma^{\gamma\alpha} - x_\gamma^{\gamma\beta}) K}{3 f_\alpha f_\beta \lambda_\alpha S^2 (x_\beta^{\beta\alpha} - x_\alpha^{\alpha\beta})} \qquad (16)$$

Similarly,

$$G_\beta = \frac{2 D_b \delta h_\beta (x_\gamma^{\gamma\alpha} - x_\gamma^{\gamma\beta}) K}{3 f_\alpha f_\beta \lambda_\beta S^2 (x_\beta^{\beta\alpha} - x_\alpha^{\alpha\beta})} \qquad (17)$$

When $G_\alpha = G_\beta$, Eq. (11) must be satisfied, and when $G_\alpha \neq G_\beta$, the inequality of Eq. (13) again results. For pearlite growing by the boundary diffusion-controlled ledge mechanism:

$$G_b = \frac{2 D_b \delta h (x_\gamma^{\gamma\alpha} - x_\gamma^{\gamma\beta}) K}{3 f_\alpha f_\beta \lambda S^2 (x_\beta^{\beta\alpha} - x_\alpha^{\alpha\beta})} \qquad (18)$$

The equations obtained here for the edgewise growth of pearlite by the ledge mechanism, Eqns. (12) and (18), differ from their Hillert (or Hillert-type) counterparts for growth by uniform atomic attachment only through multiplication by h/λ. However, this factor can readily fall in, or even below, the range 0.1-0.01 [57, 58, 59, 60, 61, 62].

The growth rate of bainite, on the other hand, is given by G_α,not by G, i.e., by Eq. (7) for D_v-control and by Eq.(16) for D_b-control. The difference between pearlite and bainite growth is particularly well illustrated by consideration of the growth kinetics of a small areal element of the α:γ boundary in the vicinity of a β crystal

which has just been surrounded by its adjacent α crystal. The average diffusion distance to the nearest β crystal is now abruptly increased. If this distance is sufficiently large, once the solute concentration gradients in the γ matrix have been rearranged, the growth rate of α will now be given by the Jones-Trivedi [51] equation:

$$G = \frac{D(x_\beta^{\beta\alpha} - x_\beta)}{\alpha\lambda(x_\beta^{\beta\alpha} - x_\alpha^{\alpha\beta})} \tag{19}$$

where α = a complex function of the composition ratio in this equation. Comparing Eq.(19) with the G_α of Eq. (7) in order to deal with two D_v-control growth processes, one observes that the ratio of the concentration differences in Eq. (7) is somewhat greater than that in Eq. (19). It is presently necessary to assume that λ_α is the same in both situations. Noting that usually $1/f_\alpha$ is a little greater than unity and that $1/\alpha$ is often somewhat less than unity, the ratio of the diffusionally-coupled to that of the diffusionally-uncoupled $G_\alpha \simeq h_\alpha/S$. From observations on eutectoid decomposition in both Ti-Cr and Fe-C-Mn [46], this ratio is appreciably less than unity, but perhaps not enough to offset greatly the reverse value of the ratios of the concentration terms in the two equations. Taken together these comparisons thus do not lead to one of these mechanisms yielding a generally distinctly faster growth rate than the other. The short, nearly constant diffusion distance characteristic of ledge growth during at least its early stages can permit uncoupled growth to match fairly well the velocity of coupled growth. Numerical calculations are accordingly required to evaluate the relative velocities of the two mechanisms in individual situations. However, this discussion does indicate that Eq. (7) (or Eq. (16)) alone is unlikely to provide a complete accounting for the growth kinetics of bainite. Further, if growth is D_b-controlled when diffusionally coupled, it may not still be so when it becomes uncoupled, thus adding the possibility of a further complication.

In respect of the assumption that equilibrium proportions of α and β have

formed, Cahn [63] has suggested on thermodynamic grounds that this is likely during eutectoid decomposition at small undercoolings. However, at large undercoolings the possibilities for non-equilibrium precipitate compositions are enhanced. Replacement of one pearlite microstructure by another, more stable pearlite has long been known [64]. It is perhaps not yet clear, however, as to whether formation of the second pearlite is driven entirely by interfacial energy minimization, as Livingston and Cahn [65] have proposed for such successive transformations in eutectoid structures, and as Tsubakino [66] has demonstrated for a cellular reaction, or by some remaining supersaturation of the product phases, as Fournelle [67] has shown to obtain during another cellular reaction sequence. If deviation from equilibrium compositions become appreciable, Eqns. (11) and (13) should be replaced by counterparts based upon comparison of the left-hand and right-hand sides of Eq.(6). Now f_α and f_β must be evaluated by quantitative metallography and $x_\beta^{\beta\alpha}$ and $x_\alpha^{\alpha\beta}$ estimated with a high resolution STEM instrument.

Returning to a position of accepting that equilibrium proportions of α and β have precipitated, we may summarize the present considerations through some modifications of Hillert's [56] description of pearlite formation as cooperative growth and of bainite formation as non-cooperative growth. On the results of Hackney and Shiflet [46], the pearlite reaction is clearly the result of *ledgewise cooperative* growth. Bainite, on the other hand, now seems to be more accurately described as *ledgewise competitive* growth. The two product phases formed during the bainite reaction compete for shares of the γ matrix, with the less successful one being repeatedly cut off from access to γ and thus being obliged to re-nucleate in order to resume its losing battle.

3.3. Kinetic Tests of These Analyses

A survey of the literature provides convincing evidence that steel--particularly when one or more alloying elements are present--is an unsatisfactory medium in which to these analyses of pearlite growth kinetics by the ledge mechanism. Partition of carbon between ferrite and carbide lamellae by both volume and interphase boundary diffusion poses problems in both mathmatical analysis which have yet to be solved and in ancillary data availability, since no success has as yet been achieved in measuring the diffusivity of carbon even in grain boundaries in either ferrite or austenite, much less at interphase boundaries in steel [68, 69], Further, when a substitutional alloying element is present, its partition behavior, though widely discussed theoretically and measured experimentally, is yet to be accounted for in a satisfactory manner [68, 69, 70].

Tests of the bainite analysis can be made in our Ti-25% Cr alloy. These are presently in progress. Results to date have been secured at one temperature. These results support the mechanism of control of growth by diffusion along the advancing interphase boundaries. Data on ledge heights and inter-ledge spacings are now being sought at other reaction temperatures in order to ascertain whether or not the conclusion initially reached is truly reliable. It should be noted here, though, that this comparison between theory and experiment is being adversely affected by the unavailability of experimental data on grain boundary diffusion, much less on interphase boundary diffusion in Ti alloys.

3.4. The Fundamental External Morphology of Bainite

Eq. (11) and the Hackney-Shiflet mechanism lead directly to pearlite morphologies which are nearly the same, except for differences in scale, in many different alloy systems. Replacement of plates by rods of the minority phase is one of the few variations found in this transformation product. In the case of bainite, however, Eq. (13), and the resulting requirement that β crystals be repeatedly

re-nucleated, yield an extraordinarily wide range of two-phase morphologies. It is thus appropriate to begin consideration of bainite morphologies with the proposal that, as in the case of pearlite, there is fundamental, essentially alloy system-independent bainite morphology. Contrary to many published views, this morphology is suggested to be the nodule, with a large disconnected dispersion of one eutectoid phase appearing within and also in contact with the "envelope" of the other eutectoid phase. When intervention by the proeutectoid phase in the development of bainite morphology is minimal, the bainite nodules should be roughly hemispherical when nucleated at grain boundary allotriomorphs of the proeutectoid phase. Nucleation of the bainite nodules at small proeutectoid phase crystals in the interiors of matrix grains should result in the formation of approximately spherical bainite nodules. An illustration at the later morphology in a hypereutectoid Ti-Cr alloy is presented in Figure 12. An equivalent morphology has been observed in hypereutectoid Fe-C alloys [71, 72]. That both observations were made in hypereutectoid alloys is not fortuitous. In both systems, the relatively small volume fraction allowed and the relatively slow transformation kinetics of proeutectoid intermetallic compound (β) as compared with those of eutectoid α minimize interference of the proeutectoid phase with the development of bainite morphology.

3.5. Internal Morphology of Bainite

Before examining the effects of proeutectoid phase interference upon bainite morphology in more detail, it is desirable to consider the possibilities for variety in the internal morphology of a bainite nodule permitted by Eq. (13). When the growth rate of eutectoid alpha is much greater than that of eutectoid beta (say), the nodules will consist of a dispersion of small eutectoid β crystals within a eutectoid α matrix. The fineness of the dispersion will increase with the ratio of the re-nucleation kinetics of eutectoid β to the growth kinetics of eutectoid α. If β crystals do not nucleate in a recognizable pattern at γ:eutectoid α boundaries, or nucleate in part

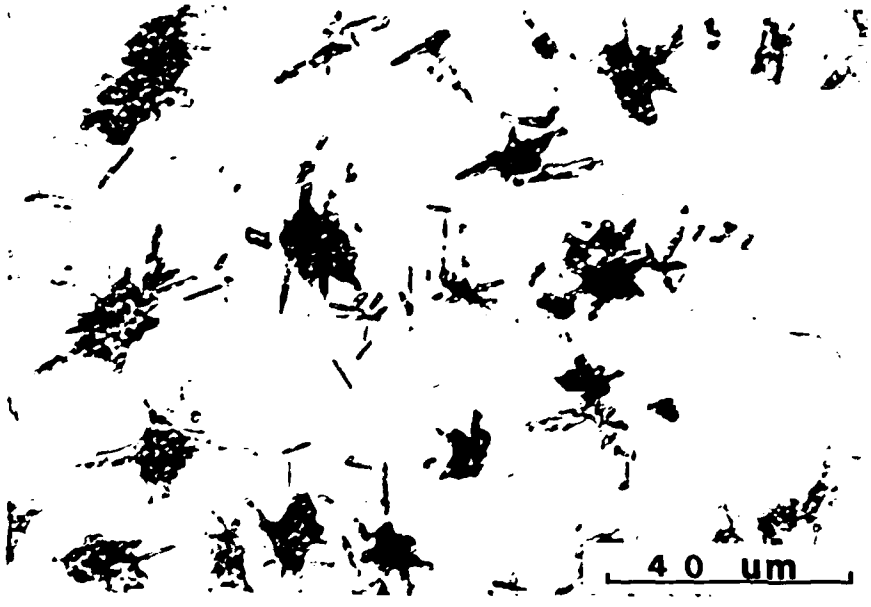

Figure 12: Optical micrograph illustrating the formation of sperical bainite nodules at proeutectoid intragranular $TiCr_2$ plates, beta sloution treated and isothermally reacted at 665°C for 5 hours. Intrgranular $TiCr_2$ plates are engulfed by bainite nodules. Etched in 20% HF, 20% HNO_3, and 60% glycerin.

within eutectoid α**, the dispersion will be approximately random. As the growth kinetics of eutectoid β approach those of eutectoid α, however, the eutectoid β crystals will become elongated in the nodule growth direction. The nodules will thus increasingly resemble pearlite. As previously indicated, unless the Hackney-Shiflet mechanism of shared growth ledges turns out to be general for pearlite, a "grey area" of morphology within which pearlite and bainite are not readily distinguishable must be accepted.

3.6. External Morphology of Bainite in the Presence of a Shape-Influencing Proeutectoid Phase

Now consider the external morphology of bainite in situation where the proeutectoid phase plays a significant role in determining the growth pattern of the bainite structure. It should first be recognized, though, that proeutectoid α is not necessarily restricted to hypoeutectoid alloys, but may also be a significant component of the microstructure in alloys of eutectoid and even of hypereutectoid composition. As examples of this statement, M. E. Nicholson [73] has deduced upon the basis of transformation kinetics considerations that proeutectoid ferrite α may be the first phase formed at higher reaction temperatures in slightly hypereutectoid eutectoid steels. Also, it presently appears that the plate-shaped bainite structures formed at lower reaction temperature in hypereutectoid Fe-C alloys are a continuation of hypoeutectoid bainite and are thus ferrite-nucleated [62, 74, 75]. And in many Ti-X systems, proeutectoid α plates form in large numbers even in alloys of approximately eutectoid composition [76].

We first examine situations in which the volume fraction of eutectoid α is markedly greater than that of eutectoid β and proeutectoid α formation preceeds the bainite reaction. Futher assume that proeutectoid α appears principally as Widmanstat-

---

**Only a proportion of the eutectoid β formable can nucleate within eutectoid α if the growth kinetics of eutectoid α do not exceed those of either direct or interfacial diffusion-aided [19] volume diffusion control.

ten sideplates and/or intragranular plates. When the incubation time for β nucleation at proeutectoid α:β boundaries is relatively long, the microstructure at late reaction times will consist predominantly of Widmanstatten α containing a limited number of β particles usually lying at α:α boundaries formed where adjacent α plates have grown into contact. Precipitation of β at γ:proeutectoid α boundaries will often permit further growth of proeutectoid α [55, 36], or the re-nucleation of α at γ:α or γ:β boundaries. The α thus formed is termed "eutectoid α". Precipitation of β particles at the interphase boundaries of parallel Widmanstatten α plates which have grown nearly into contact can permit local completion of γ decomposition by disrupting the metastable equilibrium achieved between proeutectoid α and its γ matrix. This type of microstructure is observed at higher reaction temperatures (ca. 600°C) in low alloy hypoeutectoid steels [77] and in dilute hypoeutectoid Ti-X alloys [76]. The bainitic component of this microstructure is thus a thin shealth of eutectoid α, within which a few β particles are embedded, surrounding entirely or in part some of the proeutectoid α plates formed prior to the onset of the bainite reaction.

As the nucleation rate of β in association with proeutectoid α plates (presumably still mainly at γ:proeutectoid α boundaries) increases with decreasing isothermal reaction temperature, effectively all eutectoid α plates will have β precipitates formed at their boundaries and "layers" of β alternating with further growth of eutectoid α will begin to develop. This microstructure is readily recognized as "upper bainite" in hypoeutectoid steels and Ti-X alloys [76, 77]. Even when the proportion of eutectoid α + β particles is increased appreciably with respect to that of proeutectoid α plates, the external morphology of the bainite structure is still clearly the same as that of its proeutectoid "substrate". The replacement of upper bainite by lower bainite in steel has been suggested to derive from a morphological transition [78]. Whether the change occurs in the individual ferrite plates comprising bainite sheaves, in the sheaf morphology, as a consequence, say, of a change in

sites most favorable for sympathetic nucleation [12], or both is not yet known. In any event, carbide precipitation again appears to be associated primarily with austenite ferrite boundaries [78, 79]. Thus the ferrite + carbide structures are again "plated onto" the "substrate" provided by individual ferrite plates and accordingly reflect accurately their morphology.

An equivalent situation prevails when proeutectoid α is present primarily as grain boundary allotriomorphs. This occurs, for example, when the undercooling below the $\gamma/(\alpha + \gamma)$ temperature required to form appreciable numbers of Widmanstatten plates (or needles) is not achieved until a temperature well below that of the eutectoid, or when Widmanstatten α formation is retarded by the addition of an alloying element producing a strong "solute drag-like effect" [80, 81, 82, 49, 83]. An example of the former effect may have been observed by Payson, Hodapp and Leeder [84] in plain carbon steels, at least some of which appear to have been austenitized just above their $\gamma/(\alpha + \gamma)$ temperature. The resulting very fine austenite grain size could have caused allotriomorphs of the proeutectoid phase to form instead of sideplates at temperatures just below that of eutectoid [85]. Bainitic carbide precipitation would then have occurred in association with the allotriomorphs. These experiments, however, should be repeated, with more emphasis placed upon microstructures developed during early stages of transformation and upon ensuring that carbide dissolution is always completed during the austenitizing treatment.

The precipitation of alloy carbides at the interphase boundaries of grain boundary allotriomorphs of proeutectoid ferrite in hypoeutectoid Fe-C-X alloys in which X is a strong carbide-former is well known under the name of "interphase boundary carbide precipitation" [86, 87]. The morphology of the composite bainite structure replicates that of the proeutectoid morphology from which it developed because the growth kinetics and volume fraction formable of the proeutectoid phase ferrite are high enough, so that, now acting as a eutectoid phase, it can become the

dominant partner in the eutectoid structure through continued growth, perhaps aided by sympathetic nucleation [12], of the proeutectoid ferrite allotriomorphs. When these conditions are not met, as in certain temperature-composition regions in hypereutectoid Fe-C [88, 71, 72] and Ti-Cr [89] alloys, the growth anisotropy of eutectoid α, perhaps reenforced by the influence of β precipitation on terraces between growth ledges on the migration kinetics of the risers of these ledges, can permit the eutectoid α to escape at least partially from the morphological pattern of the proeutectoid crystals at which it nucleated.

One may also consider the situation in which the proeutectoid phase in hypereutectoid alloys, here generally β, is also permitted by the Lever Rule to form a larger volume fraction of the microstructure than eutectoid α in a hypereutectoid alloy. This combination should prevail, for example, in a Ti-Cr alloy containing more than ca. 30 a/o Cr, though it has not yet been experimentally verified. The bainitic microstructures developed could be the mirror images of those considered in hypoeutectoid alloys. Thus eutectoid α crystals precipitated at the interphase boundaries of proeutectoid β plates and allotriomorphs would result in bainite structures whose external shape again reflects the morphology of their proeutectoid core.

The final type of bainite microstructure to be discussed is that in which the volume fraction of the first eutectoid phase to form is greater than that of the other low temperature phase, but the latter phase also serves as the proeutectoid phase. For example, in a eutectoid Cu-27.0 w/o Sn alloy, Spencer and Mack [64] have observed slender sideplates or needles of proeutectoid α surrounded by a much larger volume of eutectoid γ. In this situation, the growth kinetics of γ appear to be greater than those of α despite the Widmanstatten morphology of the α phase. The resulting internal microstructure does bear some resemblance to that of the proeutectoid phase. In the absence of appreciable eutectoid α nucleation at

γ:eutectoid β boundaries, however, the external morphology is markedly different from that of the other bainites so far examined. The external shape of "inverse bainite" in hypereutectoid steels [75], on the other hand, does resemble the morphology of the proeutectoid cementite plate which serves as its initial structural element. Eutectoid α nucleated at the interphase boundaries of this plate quickly engulfs it because of the much larger volume fraction of α than cementite which the phase diagram allows to precipitate. A more conventional bainite then develops from the eutectoid α. Layers of eutectoid α formed at the interphase boundaries of grain boundary cementite allotriomorphs at higher reaction temperatures in hypereutectoid steels are sometimes termed "divorced pearlite" [56]. While pearlite, rather than bainite consisting of finely divided cementite dispersed in eutectoid α, does then tend to form at γ:eutectoid α boundaries, on the present considerations the proeutectoid cementite grain boundary allotriomorphs enveloped by eutectoid ferrite interphase boundary allotriomorphs may also be fairly called bainite.

4. INTERACTION WITH STRUCTURAL MATERIALS BRANCH, MATERIALS LABORATORY, WRIGHT-PATTERSON AFB

The P.I. is presently scheduled to make three one-day visits to the Structural Materials Branch per year. His activities at WPAFB are directed and coordinated by Dr. F.H. Froes, Technical Area Manager for Titanium Programs. At this time, efforts are being made to complete the experimental work needed to prepare two technical papers, one dealing with ledge structures on sideplates of the α phase precipitated in Ti-6% Al-4% V and the other with the influence of β grain size upon the W_s temperature in this alloy. Dr. D. Eylon is in charge of the ledge growth study and Dr. A. G. Jackson is leading the grain size investigation; Dr. Froes is participating in both. In addition, Dr. Froes is serving as co-supervisor of Miss Amber Dalley's Ph.D. thesis. The P.I. continues to find these visits exceptionally stimulating. He hopes that they are proving useful to WPAFB scientists; he is finding them valuable not only in research but also in teaching activities. Even the most fundamentally oriented

metallurgy graduate students enjoy learning about practical applications of material they learn about in class.

LIST OF FIGURES

solution treated and isothermally reacted at 635°C for 3 hours. The growth ledges are spaced ca. 210 nm apart with height 25 nm. The misfit dislocations are spaced 20 nm apart between the growth ledges; b) Df micrograph showing the interfacial structures at the eutectoid $TiCr^2$:beta intefaces in the same specimen. The growth ledges are spaced ca. 30 nm apart as arrows indicated.

Figure 12: Optical micrograph illustrating the formation of sperical bainite nodules at proeutectoid intragranular $TiCr_2$ plates, beta sloution treated and isothermally reacted at 665°C for 5 hours. Intrgranular $TiCr_2$ plates are engulfed by bainite nodules. Etched in 20% HF, 20% HNO_3,and 60% glycerin.

REFERENCES

1. H.I. Aaronson , *Inst. Metals, Monogr.* , **33**, 270 (1969).
2. R. F. Hehemann, K. R. Kinsman and H. I. Aaronson , *Met. Trans.*, **3**, 1077 (1972).
3. E. S. K. Menon and H. I. Aaronson , *Mat. Sci. Forum* , **3**, 211 (1985).
4. E. S. K. Menon and H. I. Aaronson , *submitted to Acta Met., in press,* (1986).
5. E. S. K. Menon and H. I. Aaronson , *submitted to Acta Met., in press,* (1986).
6. E. S. K. Menon and H. I. Aaronson , *submitted to Acta Met., in press,* (1986).
7. E. S. K. Menon and H. I. Aaronson , *submitted to Acta Met., in press,* (1986).
8. E.S.K. Menon, M.R. Plichta and H.I. Aaronson, *Scr. Metall.*, **17**, 1455 (1983).
9. E.S.K. Menon, R.W. Hyland,Jr. and H.I. Aaronson, *Scr. Metall.*, **18**, 367 (1984).
10. V. Perovic, G.R. Purdy and L.M. Brown, *Acta Metall.*, **29**, 889 (1981).
11. V. Perovic, G.R. Purdy and L.M. Brown, *Acta Metall.*, **27**, 1075 (1979).
12. H. I. Aaronson and C. Wells, *Trans. TMS-AIME*, **206**, 1216 (1956).
13. W. Bollmann, *Crystal Defects and Crystalline Interfaces,* Springer-Verlag , Germany (1970).
14. M.G. Hall, J.M. Rigsbee and H.I. Aaronson, *Acta Met. (in press),* (1985).
15. H. I. Aaronson, *Decomposition of Austenite By Diffusional Processes,* V. F. Zackay and H. I. Aaronson, eds., Interscience, New York, 387 (1962).
16. H. I. Aaronson, C. Laird and K. R. Kinsman, *Phase Transformations,* H. I. Aaronson, ed., ASM, Metals Park, Ohio, 313 (1970).
17. H. I. Aaronson and K. C. Russell, *Proceedings of an International Conference on Solid-Solid Phase Transformations,* H. I. Aaronson, D. E. Laughlin, R. F. Sekerka and C. M. Wayman, eds., TMS-AIME, Warrendale, PA, 371 (1983).
18. H. I. Aaronson, *Trans. Indian Inst. of Metals*, **32**, 1 (1979).
19. H. B. Aaron and H. I. Aaronson, *Acta Metall.*, **16**, 789 (1968).
20. J. Goldman, H.I. Aaronson and H.B. Aaron, *Met. Trans.*, **1**, 1805 (1970).
21. A. Pasparakis, D. E. Coates and L. C. Brown , *Acta Metall.*, **21**, 991 (1973).
22. A. Pasparakis and L. C. Brown , *Acta Metall.*, **21**, 1259 (1973).
23. J. R. Bradley and H. I. Aaronson , *Met. Trans.*, **8A**, 323 (1977).
24. E.B. Hawbolt and L.C. Brown, *TMS-AIME*, **239**, 1916 (1967).
25. F.S. Ham, *Quart. of Appl. Math.*, **17**, 137 (1959).
26. G. Horvay and J.W. Cahn, *Acta Metall.*, **9**, 695 (1961).
27. G. Horvay and J.W. Cahn, Technical Report 60-RL-2561M, General Electric Research Laboratory (1960).

28. N.A. Gjostein, *Diffusion*, H.I. Aaronson, ed., ASM, Metals Park, OH, 241 (1973).

29. A.M. Brown and M.F. Ashby, *Acta Metall.*, **28**, 1085 (1980).

30. A.D. Brailsford and H.B. Aaron, *J. of App. Phys.*, **40**, 1702 (1969).

31. S. Krishnamurthy, P. G. Vogt, D. Eylon and F. H. Froes , *Proc. 1983 Powder Metallurgy Conference* , , ed., Americam Powder Metallurgy Institute, , (1983).

32. W. W. Mullins and R. F. Sekerka, *Jnl. App. Phys.* , **34**, 323 (1963).

33. W. W. Mullins and R. F. Sekerka, *Jnl. App. Phys.* , **35**, 444 (1964).

34. L. Brush and R. F. Sekerka , *Unpublished Research, Carnegie-Mellon Univ.*, (1986).

35. D. J. Delazaro and W. Rostocker , *Acta Metall.*, **1**, 674 (1953).

36. H. I. Aaronson, W. B. Triplett and G. M. Andes , *Trans. TMS-AIME*, **209**, 1227 (1957).

37. H. I. Aaronson , *Trans. Indian Inst. Metals* , **32**, 1 (1979).

38. W. F. Lang III, M. Enomoto and H. I. Aaronson , *Met. Trans., in press*, (1986).

39. J. K. Park and A. J. Ardell , *submitted to Acta Met., in press*, (1986).

40. J. K. Lee and H. I. Aaronson , *Acta Metall.*, **23**, 799 (1975).

41. J. K. Lee and H. I. Aaronson , *Acta Metall.*, **23**, 809 (1975).

42. M.R. Plichta and H.I. Aaronson, *Acta Metall.*, **28**, 1041 (1980).

43. A. D. King and T. Bell , *Met. Trans.*, **6A**, 1428 (1975).

44. R. A. Ricks and P. R. Howell , *Acta Metall.*, **31**, 853 (1983).

45. H. I. Aaronson, M. R. Plichta, G. W. Franti and K. C. Russell, *Met. Trans.*, **9A**, 363 (1978).

46. S.A. Hackney and G.J. Shiflet, *Scr. Metall.*, **19**, 757 (1985).

47. S. A. Hackney and G. J. Shiflet , *submitted to Acta Met.*, (1986).

48. M. Hillert, *Met. Trans.*, **3**, 2729 (1972).

49. M. Hillert, *The Mechanism of Phase Transformations in Crystalline Solids*, , eds., Institute of Metals, London, UK, 231 (1969).

50. J. W. Cahn, W. B. Hillig and G. W. Sears, *Acta Metall.*, **12**, 1421 (1964).

51. G.J. Jones and R. Trivedi, *J. Cryst. Growth*, **29**, 155 (1975).

52. C. Zener , *Trans. Met. Soc. AIME* , **167**, 550 (1946).

53. R. Trivedi, *Proceedings of an International Conference on Solid-Solid Phase Transformations*, H.I. Aaronson, D.E. Laughlin, R.F. Sekerka and C.M. Wayman, eds., TMS-AIME, Warrendale, PA, 477 (1983).

54. A. T. Davenport and R. W. K. Honeycombe, *Proc. Roy. Soc.*, **322**, 191 (1971).

55. A. Hultgren , *Trans. ASM.* , **39**, 915 (1947).

56. M. Hillert, *Decomposition of Austenite By Diffusional Processes,* V.F. Zackay and H.I. Aaronson, eds., Interscience, New York, 197 (1962).

57. H. I. Aaronson, J. K. Lee and K. C. Russell, *Precipitation in Solids,* K. C. Russell and H. I. Aaronson, eds., AIME, New York, 31 (1978).

58. H. I. Aaronson, *J. of Microscopy,* **102**, 275 (1974).

59. C. Laird and H.I. Aaronson, *Acta Metall.*, **15**, 73 (1967).

60. R. Sankaran and C. Laird, *Acta Metall.*, **22**, 957 (1974).

61. K. R. Kinsman, E. Eichen and H. I. Aaronson, *Met. Trans.*, **6A**, 303 (1975).

62. J.M. Howe, H.I. Aaronson and R. Gronsky, *Acta Metall.*, **33**, 649 (1985).

63. J. W. Cahn, *Acta Metall.*, **7**, 18 (1959).

64. C. W. Spencer and D. J. Mack, *Decomposition of Austenite By Diffusional Processes,* V. F. Zackay and H. I. Aaronson, eds., Interscience, New York, 549 (1962).

65. J. D. Livingston and J. W. Cahn, *Acta Metall.*, **22**, 495 (1974).

66. H. Tsubakino, *Proceedings of an International Conference on Solid-Solid Phase Transformations,* H. I. Aaronson, D. E. Laughlin, R. F. Sekerka and C. M. Wayman, eds., TMS-AIME, Warrendale, PA, 951 (1983).

67. R. A. Fournelle, *Acta Metall.*, **27**, 1147 (1979).

68. M. P. Puls and J. S. Kirkaldy, *Met. Trans.*, **3**, 2777 (1972).

69. J. W. Cahn and W. C. Hagel, *Decomposition of Austenite By Diffusional Processes,* V. F. Zackay and H. I. Aaronson, eds., Interscience, New York, 131 (1962).

70. N. Ridley, *Met. Trans.*, **15A**, 1019 (1984).

71. A. B. Greninger and A. R. Troiano, *Trans. TMS-AIME*, **140**, 307 (1940).

72. J. R. Vilella, *Trans. TMS-AIME*, **140**, 332 (1940).

73. M. E. Nicholson, *Trans. TMS-AIME*, **200**, 1071 (1954).

74. K. R. Kinsman and H. I. Aaronson, *Met. Trans.*, **1**, 1485 (1970).

75. M. Hillert, *Jernkont. Ann.*, **141**, 757 (1957).

76. G.W. Franti, J.C. Williams and H.I. Aaronson, *Met. Trans.*, **9A**, 1641 (1978).

77. S. Modin, *Jernkont. Ann.*, **142**, 37 (1958).

78. H.I. Aaronson, J. M. Rigsbee and R. Trivedi, *submitted to Scripta Met.*, (1986).

79. D. H. Huang and G. Thomas, *Met. Trans.*, **8A**, 1661 (1977).

80. H. I. Aaronson, *The Mechanism of Phase Transformations in Crystalline Solids,* , eds., Institute of Metals, London, UK, 270 (1969).

81. P. G. Boswell, K. R. Kinsman, G. J. Shiflet and H. I. Aaronson , *Proc. of Symposium in Honor of Earl Parker* , , ed., TMS-AIME, Warrendale, Pa., in press, (1986).

82. H. I. Aaronson, P. G. Boswell and K. R. Kinsman, *Proc. of Symposium in Honor of Earl Parker* , , ed., TMS-AIME, Warrendale, Pa., in press, (1986).

83. K. R. Kinsman and H. I. Aaronson, *Transformation and Hardenability in Steel*, , eds., Climax Molybdenum Co., Ann Arbor, Mich., 39 (1967).

84. P. Payson, W. L. Hodapp and J. Leeder, *Trans. ASM*, **28**, 306 (1940).

85. C. A. Dube, H. I.Aaronson and R. F. Mehl , *Rev. Met.* , **55**, 201 (1958).

86. R. W. K. Honeycombe, *Met. Trans.*, **7A**, 915 (1976).

87. R. W. K. Honeycombe, *Met. Sci. J.*, **14**, 201 (1980).

88. G. Spanos, *Unpublished Research, Carnegie-Mellon Univ., Pittsburgh, PA,* (1985).

89. H. I. Aaronson, W. B. Triplett and G. M. Andes , *Trans. TMS-AIME*, **218**, 331 (1960).

END

1-87

DTIC